Article:
Ahmed, M., Brown, S. and Cordiner, J. (2026) A generalized MILP framework for plant-level decarbonization. Energy Conversion and Management: X. 101677. ISSN: 2590-1745

https://doi.org/10.1016/j.ecmx.2026.101677

Energy Conversion and Management: X 30 (2026) 101677

Contents lists available at ScienceDirect

Energy Conversion and Management: X

journal homepage: www.sciencedirect.com/journal/energy-conversion-and-management-x

A generalized MILP framework for plant-level decarbonization

Mahdi Ahmed, Solomon Brown, Joan Cordiner *

School of Chemical, Materials & Biological Engineering, University of Sheffield, Mappin St, Sheffield, S1 4LZ, United Kingdom

ARTICLE INFO

Keywords:
Industry
Decarbonization
Sustainability
Economics
Carbon Trading
Hydrogen
Electrification
Biomass
Energy
Optimization
MILP

ABSTRACT

Energy-intensive plants must navigate technology, fuel-price, and policy uncertainty when selecting least-cost decarbonization pathways. We develop a two-stage mixed-integer linear programming (MILP) framework for industrial decarbonization planning that co-optimizes multi-technology capacity expansion and commissioning schedules with hourly site-energy dispatch, while explicitly modeling emissions-allowance procurement and intertemporal banking under an emissions trading system (ETS). The formulation combines multi-decadal investment decisions to hourly operations; includes an allowance-accounting module for ETS-consistent compliance cost calculation with banking; represents correlated trajectories for grid-carbon intensity, fuel and electricity prices, and ETS design; and incorporates time-varying technology costs for electrification, hydrogen, carbon capture and storage (CCS), and bio-energy. We demonstrate the framework on a UK epoxy-resin facility (2025–2055) under five market–policy scenarios to illustrate how scenario-driven stress-testing alters technology choice and timing. Results show that electrification is least-cost/lowest-emissions only if grid intensity falls below 50 g CO_2 kWh^{-1} by 2035; a slower trajectory increases cumulative emissions by up to 745 kt CO_2. A carbon-price corridor alone is insufficient to close the green-fuel cost premium, motivating long-dated hedging instruments (e.g., power purchase agreements and forward/swap positions) to reduce exposure to price volatility. Allowing credit banking enables additional cost-effective abatement (up to 110 kt CO_2) by valuing early over-compliance, whereas prohibiting banking increases compliance cost and weakens the cost–emissions trade-off. Overall, the framework provides a practical, scenario-driven tool for regulators and operators to evaluate robust industrial decarbonization pathways.

1. Introduction

Industrial decarbonization sits at the nexus of climate ambition and economic competitiveness. Under the Paris Agreement, signatory nations aim for net-zero greenhouse-gas emissions by mid-century; yet the industrial sector — which accounts for roughly 25 % of global CO_2 emissions and 40 % of final energy demand — remains one of the hardest to abate [1,2]. Heavy industries such as steel, cement, chemicals and refining face irreversible, high fixed costs and long asset lifetimes on thin margins. In such settings, the option value of waiting is large: firms rationally defer capital when future cash flows hinge on uncertain fuel and carbon prices, subsidy trajectories, or border measures, especially when alternative uses of capital offer lower risk and higher liquidity. Retrofitting also implies downtime and execution risk, while many low-carbon alternatives remain commercially immature or carry significant cost premia [3]. Limited consumer demand for greener products exaggerates this. Much of the value of abatement is social and does not appear in project cash flows. Credible, durableecmx101677 policies are therefore essential: predictable carbon prices, clear product and performance standards, and complementary infrastructure commitments. These instruments reduce policy and market uncertainty, narrow risk premia, lower hurdle rates, and attract investment at the plant level.

Over 20 % of worldwide industrial CO_2 emissions are now covered by cap and trade. In Europe, the EU Emissions Trading System (EU ETS), launched in 2005 and covering nearly 40 % of EU GHG emissions, has undergone sustained reforms; notably, the Market Stability Reserve (MSR) adjusts allowance supply to address surpluses and stabilize expectations [4]. The UK established the UK ETS in 2021 with its own benchmarks and trajectory. In May 2025, the EU and UK issued a Common Understanding to work toward formal ETS linkage, which would harmonize prices, deepen liquidity, and reduce compliance frictions for cross-border trade [5–7].

In parallel, the EU Carbon Border Adjustment Mechanism (CBAM) enters its definitive phase from 2026, charging embedded emissions in selected imports at the prevailing EUA price [8,9]. Linkage and the CBAM are driving a more integrated, if still evolving, carbon-pricing landscape.

* Corresponding author.
E-mail address: j.cordiner@sheffield.ac.uk (J. Cordiner).

https://doi.org/10.1016/j.ecmx.2026.101677
Received 10 October 2025; Received in revised form 19 January 2026; Accepted 12 February 2026
Available online 24 February 2026

This heightens incentives to decarbonize and the value of forward-looking decision support in the UK and EU, and similar policies are likely to diffuse internationally.

1.1. Technology pathways

Four primary decarbonization routes dominate industry road-maps, each with distinct maturity levels, infrastructure needs and cost trajectories:

- **Electrification of process heat.** Electric boilers, resistive heaters, induction furnaces and plasma torches are actively explored up to ∼500 °C. With low-carbon electricity and waste-heat recovery, lifetime OPEX savings are achievable in renewable-rich grids [10].
- **Hydrogen substitution.** Blue H_2 and green H_2 can abate on-site combustion emissions; European green H_2 costs are projected to fall materially by the 2030s with deployment and learning [11,12].
- **Carbon capture and storage (CCS).** Post-combustion amine scrubbing can remove 85–90 % of flue-gas CO_2, subject to transport and storage access; large projects report costs in the US\$60–120 t^{-1} range at scale [13].
- **Biomass and biofuels.** Sustainable biomass (pellets, residues, bio-syngas) can replace fossil fuels with low/negative lifecycle emissions such as bio-energy with CCS (BECCS), but faces feedstock and price risks [14].

Each pathway exhibits a distinct learning curve and infrastructure dependency (e.g., grid build-out, CO_2 transport and storage). Determining not only which technologies to adopt but also when to deploy them requires models that co-optimize multi-decadal investments with high-resolution operations under realistic policy signals.

1.2. Motivation and research objectives

For a given site, the least-cost route to deep decarbonization depends on the joint evolution of technology costs, electricity and fuel prices, and carbon policy design (trading rules, free allocation, banking, linkage/CBAM). Decisions are intertemporal: firms choose commissioning schedules and operating strategies, and — under an ETS — may *bank* allowances as a hedge. There is thus a need for a decision-support framework that simultaneously: (i) evaluates competing technology portfolios, (ii) optimizes the timing of investments over decades while respecting hourly operations, and (iii) represents emissions-trading compliance with intertemporal banking. This paper addresses that need.

1.3. Modeling approaches and research gaps

Mixed-integer linear programming (MILP) has become the workhorse for techno–economic studies of industrial decarbonization, at both plant and sector scales [15]. Early "first-generation" studies typically optimized process superstructures under fixed, exogenous carbon-price trajectories. For example, Huynh et al. develop a two-stage stochastic MILP for biorefinery design that compares carbon tax versus cap-and-trade policies, but treats allowance prices as external inputs and focuses on a single conversion pathway [16]. Yáñez et al. present a deterministic refinery-level CO_2 mitigation portfolio (CCS, process improvements, fuel shifts) tailored to one facility; again, policy enters only as an exogenous scenario rather than a market with trading and carry-over [17]. As Verdolini et al. emphasize in their cross-sector review, most industry models still abstract away from real market design: free allocation, banking/borrowing, or border mechanisms are often omitted [18].

"Second-generation" works begin to add multi-period planning and uncertainty. Shen et al. formulate a data-driven robust MILP for an industrial energy system with renewable integration and short-term variability, but carbon policy remains an external cap/cost without allowance trading [19]. In the cement sector, Wang et al. propose a multi-period stochastic MILP that optimizes a 30-year CCS/CCU rollout under carbon-price and capture-cost uncertainty, advancing long-horizon decisions while still centering on a single route and exogenous policy paths [20]. At the technology level, Giannikopoulos et al. study thermal electrification with onsite wind/storage in a multi-year MILP, reporting sizable emissions cuts for electric process heat, yet without considering alternative pathways or carbon market interactions [21]. Zhang et al. schedule a decade of biomass co-processing retrofits for a refinery under supply-cost uncertainty, but omit operational flexibility and emissions trading, treating carbon costs only implicitly [22]. Chew et al. co-optimize a cement plant's internal "smart energy system" with multiple technologies, though under deterministic price paths and without trading [23].

A few studies move toward more comprehensive policy representation. Guo et al. include allowance and green-certificate trading in a two-stage cement planning model and show that policy incentives can materially shift choices; however, they assume fixed stage prices and exclude banking/linkage, so compliance costs do not respond to intertemporal abatement within the model [24]. Beyond optimization, site-specific simulation frameworks such as Neuwirth et al. emulate discrete plant investment choices across energy-intensive industries under scenarios, but do not co-optimize hourly operations nor model allowance banking [25]. At the EU scale, the bottom-up FORECAST model has been used extensively to produce industrial decarbonization pathways, yet it is a simulation (not optimization) framework with exogenous carbon inputs [26]. Meanwhile, the market-design literature documents why banking matters: the EU ETS MSR alters intertemporal allowance supply and hence the value of banked permits, and agent-based/equilibrium studies show how banking and reserve rules shape price paths and investment [4,27,28]. Border measures like the EU CBAM further couple policy and trade, changing effective compliance costs for tradables [8].

Technological learning is another perspective where assumptions are often simplified. Reviews of learning highlight the importance of embedding experience curves inside the decision model, especially for planned investments in emerging options [29]. System-scale evidence shows that learning can materially shift the optimal timing and scale-up of green hydrogen, reinforcing the need to treat cost decline within long-horizon investment planning [30].

Taken together, several recurring gaps emerge across the literature reviewed above and summarized in Table 1. Carbon compliance is often represented as an exogenous CO_2 price adder or an aggregated annual penalty, with relatively few optimization studies embedding explicit scheme mechanics such as allowance balances, intertemporal banking/borrowing, or MSR-type rules [18,24]. Commodity uncertainty is frequently treated in a limited or univariate manner, despite correlations between fuel, power and CO_2 prices that can shift the relative attractiveness of competing investment options simultaneously. Finally, many studies focus on one or a small subset of routes at a time rather than scheduling investment timing across a portfolio of competing technologies within a single optimization problem [20–22].

A related modeling trade-off concerns temporal resolution. Many long-horizon planning studies simplify operations for tractability, while high-resolution operational studies typically assume fixed capacities. Hourly resolution is used here because key drivers are defined at short time scales,

Table 1
Comparison of selected industrial decarbonization optimization studies.

Study	Timing	Hourly	Multi-tech	Uncert.	Carbon policy	Horizon
Huynh et al. (2024) [16]	✗	✗	Limited	*Stoch.*	Exogenous	Design-only
Shen et al. (2022) [19]	✗	✓	Limited	*Robust*	None	Operational-only
Wang et al. (2024) [20]	✓	✗	Limited	*Stoch.*	Scenarios	**30 yr**
Yáñez et al. (2022) [17]	✗	✗	✓	*None*	None	Design-only
Giannikopoulos et al. (2024) [21]	✗	✓	Limited	*None*	None	Operational-only
Zhang et al. (2024) [22]	✓	✗	Limited	*Scen.*	Implicit	**10 yr**
Chew et al. (2025) [23]	✗	✓	✓	*None*	None	Operational-only
Guo et al. (2023) [24]	✓	✓	✓	*Scen.*	*Partial*	**2-stage (10 yr + 10 yr)**
Neuwirth et al. (2024) [25]	✓	✗	✓	*Scen.*	Scenarios	Multi-year
This work (2025)	✓	✓	✓	***Scen.***	**Trading & banking**	**30 yr**

Column definitions: *Timing* = multi-stage investment timing (capacity expansion and commissioning); *Hourly* = high-resolution operational dispatch; *Multi-tech* = portfolio of competing routes; *Uncert.* = Scenario (Scen.), Stochastic (Stoch.), Robust, or None; *Carbon policy* levels — None (ignored), Implicit (cost proxy only), Exogenous (fixed carbon path), Scenarios (policy varies by case), Partial (some trading instruments without price feedback/banking), **Trading & banking** (explicit allowance balances with intertemporal banking;
Horizon: numeric only when *Timing* is modeled; otherwise modeling scope — *Design-only* (single-shot design) or *Operational-only* (dispatch/scheduling).

including electricity prices, grid emissions intensity, operating constraints, and the availability of flexibility value streams such as demand response or load shedding [19,23]. Evaluating candidate investment pathways under hourly dispatch therefore provides a more faithful estimate of operating costs, revenues, and feasibility than purely aggregated representations, while still allowing multi-decade investment timing to be optimized.

Table 1 benchmarks representative plant/sector studies against the capabilities included here.

1.4. Scope, novelty, and structure

We develop a modular two-stage mixed-integer linear program (MILP) to support long-horizon industrial decarbonization planning under uncertain market and policy conditions. The framework combines: (i) multi-decadal capacity expansion and commissioning decisions; (ii) an ETS compliance module that tracks allowance balances over time and represents intertemporal banking under parameterized rule sets, including MSR-style mechanisms and assumptions consistent with EU–UK linkage/CBAM-style boundary conditions; (iii) correlated, scenario-based trajectories for fuel, power and CO_2 prices and ETS design, used for stress-testing rather than point forecasting; and (iv) learning-curve CAPEX dynamics for electrification, hydrogen substitution, CCS and bio-energy options. Candidate investment pathways are then assessed under hourly dispatch in Stage 2 to quantify operational feasibility and to capture short-timescale operating opportunities (including ancillary-service participation where applicable). We demonstrate the approach on a UK epoxy-resin facility (2025–2055) and evaluate five market–policy scenarios spanning grid decarbonization, commodity volatility and ETS design.

Contributions.

- Endogenous carbon compliance with banking. Allowance-accounting constraints track balances and banked credits across periods so that intertemporal compliance decisions are represented within the optimization rather than imposed externally.
- Two-stage planning with hourly dispatch assessment. Long-horizon investment timing is solved on an aggregated time grid for tractability, and the resulting capacity pathway is then assessed with *hourly* rolling-horizon dispatch to ensure operational feasibility and to quantify operating costs, revenues, and ancillary-service opportunities.
- Correlated multi-commodity uncertainty for stress-testing. Scenarios preserve cross-commodity dependencies to evaluate how simultaneous shocks in fuel, power and CO_2 prices affect investment timing and technology choice.
- Modular structure for adaptation. The compliance module is parameterized to accommodate alternative ETS designs, and the technology set can be extended with minimal reformulation, supporting transfer to other energy-intensive sites.

Paper organization.

Section 2 details the formulation, including investment and operational constraints, the allowance-balance and banking logic, scenario construction, and the computational structure adopted for tractability. Section 4 reports baseline and scenario results, including cost–emissions trade-offs and sensitivity analyses. Section 5 discusses implications and limitations and provides recommendations. Section 6 concludes and outlines extensions.

2. Methodology

2.1. Model overview

All model equations and the software implementation were developed for this study. Fig. 1 summarizes the overall workflow. The framework is formulated as a mixed-integer linear program (MILP) in Pyomo and solved using Gurobi to identify least-cost decarbonization pathways under the assumed market–policy scenario inputs. Outputs include technology investment and sizing decisions, operating schedules, and cost–emissions trade-offs.

2.2. Two-stage optimization framework

The optimization is divided into two stages (time-sequential decomposition). Stage 1 determines long-horizon investment timing and capacity expansion on a monthly grid for tractability. Stage 2 then evaluates the selected capacity pathway using hourly rolling-horizon dispatch to quantify operational feasibility and time-varying operating costs and revenues. In the present implementation, Stage 2 does not feed back to revise Stage 1 investment decisions.

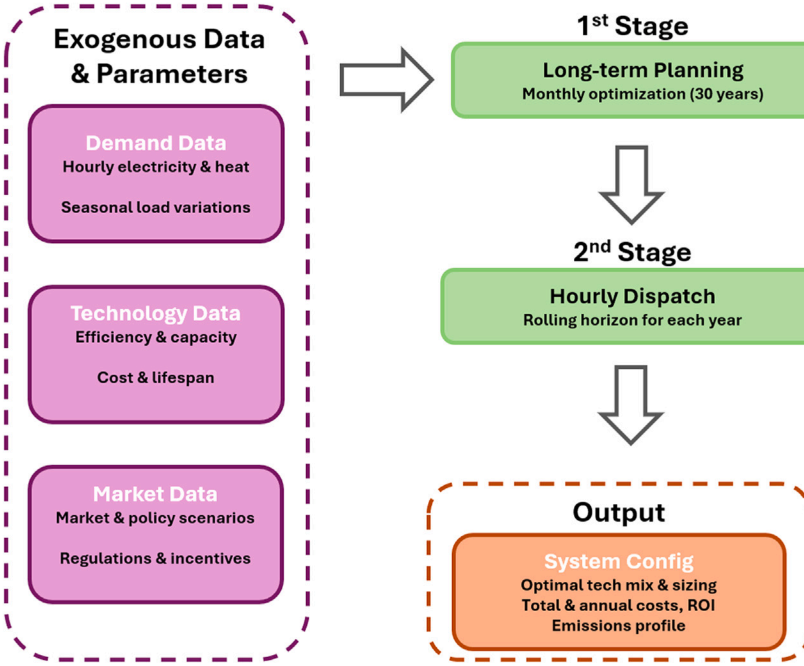

Fig. 1. Schematic representation of the integrated approach for decision-making. Inputs across demand, technology, and market variables inform the optimization. Stage 1 selects the investment pathway on an aggregated time grid, and Stage 2 evaluates the resulting capacity pathway using hourly rolling-horizon dispatch, refining operating cost/revenue estimates and capturing short-timescale operating opportunities (e.g., ancillary services).

Stage 1: Long-term investment decisions (Monthly timescale)

Stage 1 is dedicated to long-term investment decisions on a monthly basis. This stage determines the timing of capital allocation to technologies required for decarbonization. Due to the computational intensity of solving binary investment variables at hourly resolution over multi-decadal horizons, Stage 1 aggregates decisions over monthly intervals across the full investment horizon. The goal is to:

- identify which technologies to invest in (e.g., electrification, CCS, etc.);
- determine the required capacity and timing of these investments; and
- minimize the overall cost associated with fuel consumption, purchased electricity, carbon, and other relevant expenses.

Once an investment is made (e.g., electrifying a process in year 5), the new capacity becomes available and is treated as a fixed (exogenous) constraint in Stage 2. For the case study presented in this work, plant energy-service demands and product yields are specified using a fixed (stationary) operating profile over the planning horizon: demands can vary within each year to reflect typical seasonality and planned outages, but the long-run production scale and yield assumptions are not assumed to trend over time. This reflects the relatively stable throughput and utility profiles often observed at continuous chemical sites, particularly where production planning and energy procurement are supported by longer-term commercial arrangements. This is therefore a case-study specification rather than a structural limitation of the framework: if anticipated changes in throughput, yields, or product slate are available, they can be represented through time-varying demand/yield inputs, which would propagate through to investment timing and capacity choices

Stage 2: Hourly operation and dispatch (Rolling horizon)

Building upon the investment decisions from Stage 1, Stage 2 focuses on the operational aspects of the system by optimizing hourly dispatch within a rolling-horizon framework. This stage uses the capacities established in Stage 1 as exogenous inputs, so it is computationally tractable to solve the model at hourly resolution. The goals here are to:

- optimize hourly production and dispatch (based on prevailing hourly markets) to meet energy demands efficiently;
- maximize revenues from ancillary services, such as load shedding or demand-response programs;
- manage hourly operational costs, including fuel consumption, spot-market electricity purchases, and any ramping or startup/shutdown costs; and
- minimize penalties associated with shortfalls in grid reduction commitments or other obligations.

We employ a rolling-horizon approach, solving the hourly dispatch for each year sequentially across the investment horizon. As the model progresses, it incorporates the investment decisions made in Stage 1, unlocking new capacities as they become available. In the present framework, Stage 2 is used to represent operational feasibility and to quantify cost and revenue impacts at hourly resolution, but it does not feed back to revise Stage 1 investment decisions. This decoupling improves tractability for multi-decadal, multi-technology investment timing while still allowing each candidate pathway to be evaluated under hourly operating conditions. Hourly resolution is used here because key operating opportunities and constraints (including exposure to spot electricity prices and eligibility for ancillary services) are defined at short time scales. The implications of this decomposition are discussed in Section 5.

2.3. Mathematical formulation

The model partitions the site utility system into components typical of chemical plants (e.g., CHP systems, boilers, furnaces). It distinguishes between existing conventional units and units that can be adapted to alternative fuels (e.g., hydrogen, biomass) through new acquisition or retrofitting, with unit-specific cost and performance assumptions.

In this work, "biomass" refers specifically to biogas/bio-methane used as a direct substitute fuel in CHP and boiler burners, since this pathway can be represented as a relatively straightforward retrofit. We therefore do not explicitly model solid-biomass conversion routes (e.g., wood-pellet boilers) or gasification systems. Consistent with this representation, natural gas is assumed to be supplied via the conventional gas network, hydrogen via a pipeline supply option, and biogas/bio-methane via an equivalent gas-grid or dedicated supply contract (treated as an exogenous fuel price series in the model).

The core mass/energy balance and capacity constraints are common to both Stage 1 (monthly) and Stage 2 (hourly). Stage 2 additionally includes hourly throughput/dispatch detail and the ancillary-market representation, which are not required in the aggregated Stage 1 model.

2.3.1. Energy generation and procurement

This section provides constraints for Combined Heat and Power (CHP) systems (or pure heat/electric subsystems) with potential ancillary-market participation. Electrification-driven decarbonization implies that industrial producers may increasingly rely on grid electricity—raising reliability concerns if the grid itself is highly dependent on intermittent renewables [31].

An industrial site can manage reliability and cost by operating its CHP system $Q_{\text{prod}}(h)$ while also participating in ancillary (demand-response) markets [32]. This dual role (acting as both a consumer and a flexibility provider) gains economic relevance in decarbonized power systems, where supply–demand balancing becomes increasingly fragile. Industrial actors must weigh the financial incentives of demand-side participation against process downtime and internal energy needs. We enable the model to decide how much heat $Q_{\text{prod}}(h)$ to produce on-site versus how much to purchase from the grid $E_{\text{purchased}}(h)$, and how to exploit revenue streams from ancillary services $R_{\text{elec}}(h)$.

Heat Balances

The plant's *useful heat* $Q_{\text{useful}}(h)$ includes demand from storage $Q_{\text{withdrawn}}(h)$, cooling $Q_{\text{cooling}}(h)$, and new units $\sum_{t\in\mathcal{T}} Q_t(h)$. This structure lets the optimization decide if and when to invest in additional capacity $O_{\text{boiler}}(h)$ or if and when to produce steam electrically $Q_{\text{elec}}(h)$.

The thermal demand $D_{\text{heat}}(h)$ is treated as exogenous, representing a "forced" thermal load that must always be met. Eq. (3) ensures that $Q_{\text{prod}}(h)$ cannot exceed the *installed* steam-generation capacity $\left(\kappa_{\text{steam}} \times O_{\text{boiler}}(h)\right)$ plus any baseline capacity $O_{\text{baseline}}(h)$. If the model invests in more boiler capacity, the baseline operation $O_{\text{baseline}}(h)$ grows accordingly, thereby treating $Q_t(h)$ and $Q_{\text{elec}}(h)$ as exogenous in the second-stage optimization.

$$\forall h: \quad Q_{\text{useful}}(h) = \underbrace{\left(Q_{\text{withdrawn}}(h)\,\eta_{\text{withdrawal}}\right)}_{\text{steam from storage}} + \underbrace{\frac{Q_{\text{cooling}}(h)}{\text{COP}_h}}_{\text{absorption cooling load}} + \underbrace{\sum_{t\in\mathcal{T}} Q_t(h).}_{\text{load from additional units}} \tag{1}$$

$$\forall h: \quad Q_{\text{prod}}(h) + Q_{\text{elec}}(h) = Q_{\text{useful}}(h) + Q_{\text{over}}(h) - D_{\text{heat}}(h), \tag{2}$$

$$\forall h: \quad Q_{\text{prod}}(h) \leq \kappa_{\text{steam}} \times O_{\text{boiler}}(h) + O_{\text{baseline}}(h). \tag{3}$$

Electricity Balances

Eq. (4) indicates that the *net* electrical requirement $E_{\text{net}}(h)$ in hour h includes a baseline consumption $D_{\text{elec}}(h)$, plus any incremental load $Q_{\text{elec}}(h)$ if the plant decides to generate heat via electric means, minus any *reduction* $R_{\text{elec}}(h)$ provided as ancillary or demand-response service. That net load $E_{\text{net}}(h)$ is met by on-site generation $E_{\text{plant}}(h)$ and/or grid purchases $E_{\text{purchased}}(h)$. Eq. (5) splits the plant's total electrical output $E_{\text{useful}}(h)$ between *useful* consumption and any cooling $E_{\text{cooling}}(h)$ powered by electricity. Specifically, $E_{\text{useful}}(h)$ includes on-site usage $E_{\text{plant}}(h)$ plus the electrical portion of cooling $\frac{E_{\text{cooling}}(h)}{\text{COP}_e}$. Eq. (6) records any *surplus* electricity $E_{\text{over}}(h)$ as the difference between total generation $E_{\text{production}}(h)$ and the plant's useful consumption $E_{\text{useful}}(h)$.

$$\forall h \in \mathcal{H}: \quad E_{\text{plant}}(h) + E_{\text{purchased}}(h) = \left[D_{\text{elec}}(h) + Q_{\text{elec}}(h) - R_{\text{elec}}(h)\right], \tag{4}$$

$$\forall h \in \mathcal{H}: \quad E_{\text{useful}}(h) = E_{\text{plant}}(h) + \frac{E_{\text{cooling}}(h)}{\text{COP}_e}, \tag{5}$$

$$\forall h \in \mathcal{H}: \quad E_{\text{over}}(h) = E_{\text{production}}(h) - E_{\text{useful}}(h). \tag{6}$$

Ancillary Market and Flexibility Constraints

In periods of grid stress (e.g., low renewable output or high system demand), system operators may request the plant to curtail electricity consumption or provide demand response. Conversely, during times of surplus generation (e.g., very low electricity prices), the plant could shift additional processes onto electricity — such as electric boilers or other electric-driven units — to take advantage of low-cost power. We model this operational flexibility as follows:

$$\forall h \in \mathcal{H}: \quad R_{\text{elec}}(h) + R_{\text{shortfall}}(h) \geq Q_{\text{req}}(h), \tag{7}$$

$$\forall h \in \mathcal{H}: \quad R_{\text{elec}}(h) \leq \phi_{\text{flex}} \times D_{\text{elec}}(h). \tag{8}$$

Eq. (7) ensures that the sum of provided curtailment $R_{\text{elec}}(h)$ and any shortfall $R_{\text{shortfall}}(h)$ meets the grid's request $Q_{\text{req}}(h)$. Eq. (8) caps curtailment at $\phi_{\text{flex}}\, D_{\text{elec}}(h)$, preventing excessive load-shedding that could jeopardize safe operation or violate minimum production requirements. Ancillary market calls ($Q_{\text{req}}(h)$) are synthetically generated and calibrated and extrapolated against real-world data and is outlined in Appendix B.

Production and Dispatch Modeling

We assume a generic continuous production facility with no intermediate product storage. Any reduction in energy consumption (electricity or heat) directly reduces production output in that hour, and any increase in energy availability can raise output up to a nominal maximum. Let $\psi(h)$ denote the production throughput (e.g., mass or volume per hour) in hour h. We link net available energy to output via a linear relation:

$$\forall h \in \mathcal{H}: \quad \psi(h) \;=\; \phi_{\text{prod}}\Big[E_{\text{purchased}}(h) + D_{\text{heat}}(h) - R_{\text{elec}}(h) - R_{\text{heat}}(h)\Big]. \tag{9}$$

If both $E_{\text{purchased}}(h)$ and $D_{\text{heat}}(h)$ are fully met, $\psi(h)$ can reach its nominal maximum. If the plant decides to curtail electricity $R_{\text{elec}}(h)$ to satisfy an ancillary-service call or because grid prices spike, production $\psi(h)$ declines proportionally according to Eq. (9).

1. Any energy curtailment reduces production output, assuming no intermediate storage buffering.
2. If electricity prices are low enough relative to production margins, the plant may choose to increase $E_{\text{purchased}}(h)$ (and, where available, shift heat generation to electric boilers).
3. Full-plant shutdowns are avoided by capping ϕ_{flex} at a safe fraction (e.g., 10 %–20 %) of demand, reflecting that only partial curtailment is feasible without jeopardizing safety or violating long-term contracts.

By directly linking production to net energy availability, the model captures both (i) the plant's ability to provide ancillary services and (ii) its opportunistic ramp-up of electricity-intensive processes during periods of low energy cost. This general framework applies to any continuous process that scales production with available electricity and heat.

Note that these equations are subject to additional weather-related assumptions and constraints which are expanded upon in Appendix C.

Refrigeration Balances

Eqs. (10)–(11) model a trigeneration concept (CHPC), where both thermal $Q_{\text{prod}}(h)$ and electrical $E_{\text{production}}(h)$ energies can be used for cooling processes. Surplus or "waste" heat $Q_{\text{over}}(h)$ can thus reduce electrical cooling requirements $E_{\text{cooling}}(h)$, optimizing overall energy use.

$$\forall h \in \mathcal{H}: \quad R_{\text{prod}}(h) \;=\; E_{\text{cooling}}(h)\,\text{COP}_e \;+\; \Delta H_{\text{cooling}}(h)\,\text{COP}_h, \tag{10}$$

$$\forall h \in \mathcal{H}: \quad R_{\text{prod}}(h) \;=\; D_{\text{refrigeration}}(h). \tag{11}$$

Ramping Constraints

Eqs. (12)–(13) ensure that the CHP system's heat production $Q_{\text{prod}}(h)$ does not exceed technical limitations on how quickly it can increase or decrease between consecutive hours. Specifically, $R_{\text{up}}(h)$ and $R_{\text{down}}(h)$ represent the maximum allowable ramp-up and ramp-down rates, respectively.

$$\forall h \in \mathcal{H}\setminus\{0\}: \quad Q_{\text{prod}}(h) \;-\; Q_{\text{prod}}(h-1) \;\leq\; R_{\text{up}}(h), \tag{12}$$

$$\forall h \in \mathcal{H}\setminus\{0\}: \quad Q_{\text{prod}}(h-1) \;-\; Q_{\text{prod}}(h) \;\leq\; R_{\text{down}}(h). \tag{13}$$

CHP Production Relationships

Eq. (14) defines the electricity output $E_{\text{production}}(h)$ as a function of the fraction ρ_{energy} of the total heat production $Q_{\text{prod}}(h)$ that is allocated to electrical conversion, modulated by the electrical efficiency $\eta_{\text{electrical}}(h)$. For systems dedicated exclusively to heat or electricity generation, one can set $\rho_{\text{energy}} = 0$ or $\rho_{\text{energy}} = 1$ respectively, resulting in a degenerate case. Eq. (15) establishes the relationship between total heat production $Q_{\text{prod}}(h)$ and the fuel consumed $F_{\text{consumed}}(f,h)$ allocated for utilities generation. The term $\frac{HHV_f}{\Delta H_{\text{steam}}}$ converts the Higher Heating Value (HHV) of fuel f into steam energy, while $B_f(f,h)$ represents the blend ratio of fuel f at time h. The factor $(1-\rho_{\text{energy}})$ allocates the remaining heat production to thermal processes, adjusted by the thermal efficiency $\eta_{\text{thermal}}(h)$. Eq. (16) enforces that the sum of fuel blend ratios $B_f(h)$ for all fuels $f \in \mathcal{F}$ equals 1, ensuring a valid fuel mixture.

$$\forall h \in \mathcal{H}: \quad E_{\text{production}}(h) \;=\; \Big(Q_{\text{prod}}(h)\,\rho_{\text{energy}}\Big) \;\times\; \eta_{\text{electrical}}(h), \tag{14}$$

$$\forall h \in \mathcal{H}: \quad \sum_{f\in\mathcal{F}}\Big[\frac{HHV_f}{\Delta H_{\text{steam}}} \times B_f(f,h) \;\times\; F_{\text{consumed}}(f,h)\Big] \;\times\; \big(1-\rho_{\text{energy}}\big) \;\times\; \eta_{\text{thermal}}(h) \;=\; Q_{\text{prod}}(h), \tag{15}$$

$$\forall h \in \mathcal{H}: \quad \sum_{f\in\mathcal{F}} B_f(h) = 1, \quad 0 \;\leq\; B_f(h) \;\leq\; 1. \tag{16}$$

CHP Efficiencies

We model the electrical $\eta_{\text{electrical}}(h)$ and thermal $\eta_{\text{thermal}}(h)$ efficiencies of a CHP system as functions of the fuel blend ratios $B_f(h)$, ambient temperature $T_{\text{ambient}}(h)$, and other operational parameters. Fuel blend ratios directly influence both electrical and thermal efficiencies by altering combustion properties and flame dynamics [33]. Additionally, higher ambient temperatures can reduce thermal gradients, decreasing overall system efficiency [34].

We can write:

$$\forall h \in \mathcal{H}: \quad \eta_{\text{elec}}(h)\,C_{\text{CHP}} \;=\; \sum_{f\in\mathcal{F}} B_f(h)\Big[\alpha_{\text{elec},f}\,C_{\text{CHP}} \;+\; \beta_{\text{elec},f}\,E_{\text{production}}(h) \;+\; \gamma_{\text{elec},f}\,T_{\text{ambient}}(h)\,C_{\text{CHP}}\Big]. \tag{17}$$

Eq. (17) shows how the electrical efficiency $\eta_{\text{electrical}}(h)$ depends on the weighted contribution of each fuel f through the blend ratios $B_f(h)$. Each term inside the summation includes:

- A base capacity effect: $\alpha_{\text{elec},f}\,C_{\text{CHP}}$,
- A production-load dependence: $\beta_{\text{elec},f}\,E_{\text{production}}(h)$,
- An ambient-temperature impact: $\gamma_{\text{elec},f}\,T_{\text{ambient}}(h)\,C_{\text{CHP}}$.

Similarly, the thermal efficiency $\eta_{\text{thermal}}(h)$ can be modeled as:

$$\forall h \in \mathcal{H}: \quad \eta_{\text{thermal}}(h)\, C_{\text{CHP}} = \sum_{f \in \mathcal{F}} B_f(h) \left[\alpha_{\text{therm},f}\, C_{\text{CHP}} + \beta_{\text{therm},f}\, Q_{\text{prod}}(h) + \gamma_{\text{therm},f}\, T_{\text{ambient}}(h)\, C_{\text{CHP}} \right]. \tag{18}$$

Eq. (18) captures the thermal efficiency $\eta_{\text{thermal}}(h)$'s dependence on fuel blend ratios $B_f(h)$, operational load $Q_{\text{prod}}(h)$, and ambient temperature $T_{\text{ambient}}(h)$. The parameters $\alpha_{\cdot,f}$, $\beta_{\cdot,f}$, and $\gamma_{\cdot,f}$ should be derived from manufacturer data, empirical fits, or process simulations, indicating how capacity C_{CHP}, ambient conditions $T_{\text{ambient}}(h)$, and load levels $Q_{\text{prod}}(h)$ influence overall thermal efficiency.

$$\forall h \in \mathcal{H} \setminus \{0\}, \quad Q_{\text{stored}}(h) = \lambda \cdot \big(Q_{\text{stored}}(h-1) + (Q_{\text{over}}(h) \cdot \eta_{\text{storage}}) - (Q_{\text{withdrawn}}(h)/\eta_{\text{withdrawal}})\big) \tag{19}$$

$$\forall h \in \mathcal{H}, \quad Q_{\text{stored}}(h) \le Q_{\text{max, storage}} \tag{20}$$

The heat storage dynamics within the system are described by Eqs. (19) and (20), assuming a large hot water tank. Eq. (19) calculates the stored heat $Q_{\text{stored}}(h)$ at each hour by integrating heat contributions from over-production $Q_{\text{over}}(h)$ and subtracting withdrawals $Q_{\text{withdrawn}}(h)$, adjusted for storage efficiency η_{storage}, withdrawal efficiency $\eta_{\text{withdrawal}}$, and inherent system losses represented by the decay factor λ per time step. Eq. (20) sets an upper limit $Q_{\text{max, storage}}$ on the heat that can be stored.

2.3.2. Investment timing modeling

We allow single-event or multi-stage investments. Future technologies like auxiliary boilers or retrofit CHP units can be capital-intensive, and operators often delay or stage investments to mitigate large up-front costs [35]. This approach also accounts for the potential learning-curve benefits (such as cost reductions or performance improvements in hydrogen systems) where cost trends heavily influence timing decisions [36]. Delaying or distributing investments can act like an insurance policy against technology obsolescence or market volatility, optimizing project viability by balancing near-term risk with longer-term gains. In many real-world scenarios, capital-intense expansions are pursued only when projected returns justify the risk, reinforcing the need for an explicit "investment timing" sub-model within broader decarbonization optimization.

Exogenous CAPEX trajectories

All capital costs for new technologies (e.g., electrolyzers, CCS units, electric boilers, biomass retrofits) are based on *exogenous*, time-dependent unit cost trajectories rather than being derived endogenously from cumulative capacity. Specifically, for each technology t and investment interval m, we define:

$$\text{CAPEX}_t(m) = C_t^{\text{unit}}(m) \times x_t(m),$$

Thus, the total CAPEX term in the Stage 1 objective is:

$$\sum_{m \in \mathcal{M}} \sum_{t \in \mathcal{T}} C_t^{\text{unit}}(m)\, x_t(m).$$

By using an exogenous unit cost trajectory $C_t^{\text{unit}}(m)$, the model captures expected cost reductions (e.g., due to global learning or economies of scale). If $C_t^{\text{unit}}(m)$ drops over m, the optimizer will naturally delay or stage investments to take advantage of lower future costs.

1. Single-event (one-time) investment

In certain cases, the plant may only invest *once* over a multi-period horizon, deciding *when* (i.e., in which month or other time interval) to incur the capital cost $x_{\text{invest},t}(m)$, for instance, to retrofit an existing system or perform a complete replacement.

Eq. (21) states that if $x_{\text{invest},t} = 1$, exactly one interval invests: the sum of $x_{\text{invest},t}(m)$ across all $m \in \mathcal{M}$ is 1. If $x_{\text{invest},t} = 0$, the plant never invests, so all $x_{\text{invest},t}(m) = 0$. Eq. (22) ensures $x_{\text{active},t}(m) = 1$ if an investment has occurred in any prior or current interval $j \le m$; once installed, the technology remains active thereafter. Eq. (23) ensures that the technology's operational output $O_t(m)$ cannot exceed its capacity $\overline{C}_t$ if it is not active.

This approach is ideal when only *one* discrete purchase is permitted (e.g., an expensive system that is either "all or nothing"), and the model must determine the *optimal timing* of that single investment.

$$\sum_{m \in \mathcal{M}} x_{\text{invest},t}(m) = x_{\text{invest},t}, \tag{21}$$

$$\forall t \in \mathcal{T}, \forall m \in \mathcal{M}: \quad x_{\text{active},t}(m) = \sum_{\substack{j \in \mathcal{M}: \\ j \le m}} x_{\text{invest},t}(j), \tag{22}$$

$$\forall t \in \mathcal{T}, \forall m \in \mathcal{M}: \quad O_t(m) \le \overline{C}_t \cdot x_{\text{active},t}(m). \tag{23}$$

If multiple *types* of single-event technologies are allowed (e.g., hydrogen system $x_{\text{invest}}^{(\text{H2})}$, electric boiler $x_{\text{invest}}^{(\text{EB})}$, or CCS $x_{\text{invest}}^{(\text{CCS})}$) but only one can be chosen:

$$x_{\text{invest}}^{(\text{H2})} + x_{\text{invest}}^{(\text{EB})} + x_{\text{invest}}^{(\text{CCS})} \le 1, \tag{24}$$

ensuring that at most one technology is selected for investment across the entire horizon.

2. Multi-stage (cumulative) investment

In contrast, the plant may *incrementally expand* capacity or acquire multiple units over multiple time periods, resulting in cumulative installed capacity over time.

Cumulative Investment Constraints:

$$\forall\, m \in \mathcal{M},\ \forall\, t \in \mathcal{T}:\quad A_{\text{tech}}(m,t) = \begin{cases} x_{\text{purchase}}(0,t), & \text{if } m = 0, \\ A_{\text{tech}}(m-1,t) + x_{\text{purchase}}(m,t), & \text{if } m > 0, \end{cases} \tag{25}$$

$$\forall\, t \in \mathcal{T}:\quad I_{\text{tech}}(t) = \sum_{m\in\mathcal{M}} x_{\text{purchase}}(m,t), \tag{26}$$

$$\forall\, m \in \mathcal{M},\ \forall\, t \in \mathcal{T}:\quad O_{\text{tech}}(m,t) \le C_{\text{installed}}(t) \cdot A_{\text{tech}}(m,t), \tag{27}$$

$$\sum_{t\in\mathcal{T}} C_{\text{installed}}(t) \le R_{\max}. \tag{28}$$

Eq. (25) defines $A_{\text{tech}}(m,t)$, the installed capacity of technology t in period m. If a purchase occurs at $m = 0$, that technology is available immediately; otherwise, capacity grows as $x_{\text{purchase}}(m,t)$ decisions are made. Eq. (26) accumulates all purchases of technology t over the horizon, yielding a total investment measure $I_{\text{tech}}(t)$. Eq. (27) ties operational output $O_{\text{tech}}(m,t)$ to the product of installed capacity factor $A_{\text{tech}}(m,t)$ and per-unit capacity $C_{\text{installed}}(t)$, ensuring no technology exceeds its installed capacity. Eq. (28) imposes a system-wide limit $R_{\max}$ on total nominal capacities, reflecting resource or budget caps.

If each investment decision is binary (install or not), then $x_{\text{purchase}}(m,t)$ and $A_{\text{tech}}(m,t)$ can be constrained to $\{0,1\}$.

This formulation can be adapted for:

- **Auxiliary boilers**, where $x_{\text{purchase}}(m,t)$ triggers new heat-generation capacity.
- **Hydrogen technologies**, such as electrolyzers $x_{\text{purchase}}(m,t)$ or fuel cells $x_{\text{purchase}}(m,t)$, with staged expansions.
- **Retrofits of existing plants**, where partial upgrades $x_{\text{purchase}}(m,t)$ become available immediately upon purchase.

2.3.3. Carbon trading and CCS

Participation in ETS requires firms to either reduce their emissions or purchase carbon allowances $C_{\text{credits}}(i)$ and offsets $C_{\text{offset}}(i)$. In this model, we focus primarily on the use of carbon credits and abatement through CCS, and ultimately, find a way to manage long-term cost uncertainty while navigating increasingly stringent carbon pricing regimes and reducing the economic cost of compliance. Due to the UK/EU ETS linkage, this study assumes fungible carbon credits and identical prices across both markets, and that this UK plant therefore follows the pattern of the larger EU market.

Under full ETS linkage, no additional CBAM surcharge applies to exports within the UK/EU. If the plant exported to a non-linked jurisdiction, a CBAM-equivalent fee (equal to the prevailing EU ETS price) would be added; we do not explicitly model CBAM certificates beyond this optional surcharge.

Allowance allocation, purchase and banking

At each planning interval $i \in \mathcal{I}$, the plant is granted $C_{\text{free}}(i)$ allowances and emits a net $E_{\text{uncaptured}}(i)$ tonnes of CO_2 after any capture. To comply with the EU/UK ETS, the plant must surrender exactly $E_{\text{uncaptured}}(i)$ allowances, which it can cover using its free allocation $C_{\text{free}}(i)$, any previously banked allowances $C_{\text{bank}}(i-1)$, and additional market purchases $C_{\text{credits}}(i)$. If the sum of free allowances and banked credits exceeds actual emissions, the surplus can either be carried forward in the bank $C_{\text{bank}}(i)$ or sold $C_{\text{sold}}(i)$ in subsequent intervals.

Balance and Banking Constraints

Eq. (29) guarantees that total surrendered allowances (free, banked, or bought) cover the plant's emissions. Eq. (30) defines the "earned" surplus when emissions fall below available allowances; the binary $\beta(i)$ and Big-M constraints in Eq. (31) ensure that in each period the plant either purchases *or* earns/banks, but not both. Eq. (32) caps sales by what is in the bank, and Eq. (33) carries forward any unused allowances (free or purchased) net of sales.

$$\forall i:\quad C_{\text{free}}(i) + C_{\text{bank}}(i-1) + C_{\text{credits}}(i) \ \ge\ E_{\text{uncaptured}}(i), \tag{29}$$

$$\forall i \setminus \{0\}:\quad C_{\text{earned}}(i) = \big[C_{\text{free}}(i) + C_{\text{bank}}(i-1) - E_{\text{uncaptured}}(i)\big]\big[1-\beta(i)\big], \tag{30}$$

$$\forall i:\quad C_{\text{credits}}(i) \le M\,\beta(i), \quad C_{\text{earned}}(i) \le M\,[1-\beta(i)], \tag{31}$$

$$\forall i \setminus \{0\}:\quad C_{\text{sold}}(i) \le C_{\text{bank}}(i-1) + C_{\text{earned}}(i), \tag{32}$$

$$\forall i:\quad C_{\text{bank}}(i) = C_{\text{bank}}(i-1) + C_{\text{earned}}(i) + C_{\text{credits}}(i) - E_{\text{uncaptured}}(i) - C_{\text{sold}}(i). \tag{33}$$

Credit disposal

Real-world ETS frequently impose rules that limit how long surplus allowances may be held before they must be surrendered for compliance or sold. These delayed-disposal restrictions shape firms' investment strategies: a plant that anticipates tighter future caps or higher carbon prices may wish to *bank* allowances now for later use, yet mandatory disposal deadlines constrain inter-temporal arbitrage and can force earlier liquidation. We embed a *maximum holding period* $T_{\max}$, stipulating that allowances obtained in interval i must be utilized or sold no later than interval $i+T_{\max}$, for flexibility to reflect potential policy scenarios.

We introduce a continuous decision variable $D_{i,j} \ge 0$ indicating the amount of credits *earned* in interval i that are *disposed* (either sold or used to offset emissions) in interval j. The total credits earned in interval i are denoted $C_{\text{earned}}(i)$, and the model must allocate these earned credits to disposal intervals within the allowed range.

$$\mathcal{D} = \big\{(i,j)\,\big|\, i,j \in \mathcal{I},\ j \ge i,\ j \le i + T_{\max}\big\}.$$

Eq. (34) enforces that *all* credits earned in interval i are eventually disposed of, and none can remain on the books beyond $T_{\max}$ intervals. For each disposal interval j, the sum of incoming disposals from all possible origins i (where j is within the allowed disposal window for i) must match the total credits sold or used to offset in j.

$$\forall i \in \mathcal{I}:\quad \sum_{\substack{j\in\mathcal{I}:\\ j\ge i,\ j\le i+T_{\max}}} D_{i,j} = C_{\text{earned}}(i). \tag{34}$$

$$\forall j \in \mathcal{I}: \quad \sum_{\substack{i \in \mathcal{I}: \\ i \le j,\, j \le i+T_{\max}}} D_{i,j} \;=\; C_{\text{sold}}(j) + C_{\text{offset}}(j). \tag{35}$$

Eq. (35) ensures that the total credits *disposed* in interval j exactly matches the sum of those used for offsetting or sold on the market.

With the ETS, compliance cycles and auction schedules can limit the banking of allowances across multiple phases, especially if the scheme undergoes periodic cap revisions or expansions.

Carbon capture and storage

Carbon Capture and Storage (CCS) provides a route to on-site abatement by diverting a portion of flue gas to an amine-based solvent system. The Operational Expenditure (OPEX) in amine-based CCS systems is primarily driven by the *reboiler duty* $Q_{\text{CCS}}(h)$ required to strip CO_2 from the solvent, which constitutes a significant portion of the energy consumption [37]. Studies have shown that the reboiler duty can account for up to 60 %–70 % of the total OPEX, making it a critical factor in the economic viability of CCS [38].

Moreover, utilizing waste heat for the reboiler can significantly lower operating costs by reducing the reliance on external heat sources [39]. This makes the reboiler duty an ideal target for optimization, as integrating waste heat recovery into the CCS process can improve overall efficiency of industrial sites [40].

Let $E_{\text{CO}_2}(h)$ denote the raw CO_2 emissions if no capture occurs in hour h. We define:

$$E_{\text{captured}}(h) = \kappa_{\text{cap}}(h) \;\cdot\; E_{\text{CO}_2}(h), \tag{36}$$

$$Q_{\text{CCS}}(h) = \alpha_A \; E_{\text{captured}}(h) \;+\; \alpha_B \; \frac{\kappa_{\text{cap}}(h)}{1 - \gamma_{ccs}\, \kappa_{\text{cap}}(h)}. \tag{37}$$

Here, $\kappa_{\text{cap}}(h) \in [0, 1]$ is the fraction of CO_2 captured. The term $\alpha_A\, E_{\text{captured}}(h)$ models a linear re-boiler load, while the second term introduces a ***nonlinear*** escalation as $\kappa_{\text{cap}}(h)$ approaches 1 (i.e., near-total capture demands disproportionately higher energy). This encourages the solver to find an *optimal* capture fraction (e.g., 85 %–90 %) unless carbon prices justify pushing beyond that threshold. Non-linear elements are linearized piecewise.

Uncaptured CO_2

Reducing $E_{\text{uncaptured}}(h)$ lowers the plant's compliance cost. If the plant invests in *auxiliary boilers* to supply CCS steam, those boilers' emissions $E_{\text{CO}_2,\text{boiler}}(h)$ are all assumed to go uncaptured, adding to $E_{\text{uncaptured}}(h)$.

$$E_{\text{uncaptured}}(h) \;=\; E_{\text{CO}_2}(h) \;-\; E_{\text{captured}}(h) \;+\; (\text{extra flue gas if new boilers are fossil-based}). \tag{38}$$

High capture rates require more steam for solvent regeneration. Let $A_{\text{boiler}}(m)$ denote the cumulative boiler capacity in period m, with investment decisions $P_{\text{purchase,boil}}(m) \ge 0$ adding new capacity:

$$A_{\text{boiler}}(m) = A_{\text{boiler}}(m-1) \;+\; P_{\text{purchase,boil}}(m), \quad A_{\text{boiler}}(0) = 0. \tag{39}$$

At an hourly resolution h, total steam production $Q_{\text{prod}}(h)$ must remain within available capacity:

$$Q_{\text{prod}}(h) \;\le\; O_{\text{boiler}}(h), \tag{40}$$

where $O_{\text{boiler}}(h)$ represents the actual operation level. This coupling ensures the plant cannot capture large amounts of CO_2 without also securing adequate steam.

If captured CO_2 is sequestered underground, the model effectively treats those emissions as zero on-site. Policy frameworks in some jurisdictions differ on whether carbon in the ground" (e.g., geological storage) entitles the operator to additional credits (negative emissions) or merely zero-rates them [41]. Our baseline approach is to reduce on-site $E_{\text{CO}_2}(h, s)$ proportionally by κ_{cap}, thus lowering the net $E_{\text{uncaptured}}(h)$". Parameters involved in these constraints are shown in Appendix Table 13.

2.4. Carbon price solver

We implement a carbon-price solver to determine, for each year t, the EU-ETS allowance price $p(t)$ that would theoretically clear the market given each plant's optimal decarbonization response as a sensitivity tool, applying it to scenarios in which decarbonization is limited or delayed, so that we can identify the threshold carbon prices needed to trigger abatement and quantify their feedback on the market itself.

Market-Clearing Equations

$$\widetilde{C}_{\text{auc}}(t) = C_{\text{auc}}(t) - R(t), \qquad \text{(net auction supply after MSR withdrawals)}, \tag{41}$$

$$B(t) = B(t-1) + \widetilde{C}_{\text{auc}}(t) - E\big(t, p(t)\big), \qquad \text{(update of the sector's bank of unused allowances)}, \tag{42}$$

$$R(t+1) = \phi_{\text{MSR}}\; \max\big(0,\; B(t) - \Theta\big), \qquad \text{(MSR withdrawal when bank exceeds threshold)}. \tag{43}$$

Eq. (41) computes the net volume of allowances offered at auction in year t once MSR withdrawals $R(t)$ have been removed. Eq. (42) updates the cumulative bank $B(t)$ by adding net auction supply and subtracting actual emissions $E(t, p(t))$. Eq. (43) defines the MSR withdrawal rule: if the bank $B(t)$ exceeds the threshold Θ, a fraction ϕ_{MSR} of the excess is removed; the max ensures no negative (i.e. no injection).

The market-clearing problem defined by Eqs. (41)–(43) is solved numerically with the bisection-style procedure in Algorithm 1 shown in Appendix D.4. For each simulation year the algorithm adjusts the EU-ETS allowance price until aggregate emissions from all plants equal the net auction supply after MSR withdrawals. During the search it also pin-points the *floor* (the lowest price below which cheaper allowances no longer raise emissions) and the *ceiling* (the highest price above which allowances no longer induce additional abatement), thus identifying the price plateau on which plant-level decisions become market inefficient.

Throughout Section 4, we use this solver as a sensitivity tool: in scenarios where abatement is delayed or physically constrained, we vary only the MSR withdrawal rule and infer the consistent price trajectory $p(t)$. This aims to reveal the carbon-price stringency required to unlock abatement under such bottlenecks, while quantifying the feedback onto the allowance bank and MSR actions.

2.4.1. Correlated market trajectories

We develop a scenario generator (Appendix A) to generate, multi-commodity price trajectories that preserve observed cross-commodity correlations. Each commodity's base price evolves according to a "decarbonization wedge" formula—compound escalation for natural gas and biomass, decline for electricity and hydrogen, which are adjusted by deterministic seasonality and stochastic volatility shocks whose magnitudes reflect renewable penetration. Time-varying correlation factors blend related commodities (e.g., hydrogen prices increasingly track electricity as renewables scale), and discrete policy or event multipliers (e.g., short-term supply shocks) are applied when specified. All resulting price series are then passed exogenously into the model.

2.4.2. Objective functions

The objective functions for both stages are presented below, capturing CAPEX, OPEX, and revenue from ancillary-market participation and production.

Stage 1: Investment & cost (monthly)

Stage 1 focuses on determining the optimal investment decisions and minimizing the associated monthly costs. These investment decisions form the foundation for subsequent stages by establishing the capacities and configurations that will influence operational and contractual optimizations.

We define the total monthly cost $\mathcal{Z}$ across all months $m \in \mathcal{M}$ as follows:

$$\begin{aligned}
\min \quad \mathcal{Z}_1 = \sum_{m\in\mathcal{M}} \Bigg[& \underbrace{\sum_{f\in\mathcal{F}} B_f(m)\, F_{\text{consumed}}(m)\, \mathrm{P_f}(f,m)}_{\text{(1) Fuel Cost}} + \underbrace{\Big(E_{\text{purchased}}(m)\, \mathrm{P}^{\text{buy}}_{\text{elec}}(m) - E_{\text{sold}}(m)\, \mathrm{P}^{\text{sell}}_{\text{elec}}(m)\Big)}_{\text{(2) Net Electricity Cost}} \\
& - \underbrace{Q_{\text{over}}(m)\, \mathrm{P}^{\text{sell}}_{\text{heat}}(m)}_{\text{(3) Heat Revenue}} + \underbrace{C_{\text{credits}}(m)\, \mathrm{P}_{\text{credit}}(m)}_{\text{(4) Carbon Compliance Cost}} + \underbrace{C_{\text{sold}}(m)\, \mathrm{P}_{\text{credit}}(m)}_{\text{(5) Carbon Credit Revenue}} \\
& + \underbrace{\Big[\alpha_{\text{amine}} + \alpha_{\text{liquid}} + \alpha_{\text{transport}}\Big] C_{\text{captured}}(m)}_{\text{(6) CCS Operational Expenditure}} \Bigg] \\
& + \underbrace{\sum_{m\in\mathcal{M}} \sum_{t\in\mathcal{T}} x_{\text{purchase}}(m,t)\, \mathrm{CAPEX}_t(m,t)}_{\text{(7) Multi-Period Investment Costs}} \\
& + \underbrace{\sum_{m\in\mathcal{M}} \sum_{t\in\mathcal{T}} x_t(m,t)\, \mathrm{CAPEX}_t(m,t)}_{\text{(8) Single-Decision Investment Costs}} .
\end{aligned} \tag{44}$$

This objective function ensures that investment and operational costs are minimized, while maximizing profit from production.

Stage 2: Ancillary and production revenues

Building on the investment decisions from Stage 1, Stage 2 optimizes operational strategies on an hourly basis within a rolling horizon framework. Here, investment variables are treated as exogenous, allowing for the maximization of operational revenues. The objective is to maximize net revenues, which include production and ancillary revenues while accounting for penalties.

Note that the total calculated costs (taken as $\mathcal{Z}_1$) in this stage mirrors stage 1, except that it is instead subtracted and evaluated on an hourly basis.

$$\max \quad \mathcal{R} = \sum_{h\in\mathcal{H}} \Big[\underbrace{\psi(h) \times P_{resin}(h)}_{\text{(1) Production Revenue}} + \underbrace{\mathrm{P}_{\text{reward}}(h) \times R_{\text{elec}}(h)}_{\text{(2) Ancillary Revenue}} - \underbrace{\mathrm{P}_{\text{penalty}}(h) \times R_{\text{shortfall}}(h)}_{\text{(3) Shortfall Penalty}} - \mathcal{Z}_1 \Big] . \tag{45}$$

By maximizing net revenues, Stage 2 ensures optimal operational performance based on the investment framework established in Stage 1.

3. Case study: Epoxy resin production at a UK chemical plant

This study examines a UK-based chemical plant that produces **Epoxy Resin**, a high-value specialty polymer used in composites and coatings.

3.1. Plant and process overview

We consider a representative 100 000 t yr^{-1} epoxy-resin plant. Important features are outlined below:

- **Reaction and Heating:** Epoxy polymerization occurs at 250–300 °C, all process heat being supplied by a high-pressure steam network, backed by an integrated heat-storage tank for peak-load shaving and outage resilience.
- **Continuous Operation:** The plant runs 24/7, with a planned maintenance outage of approximately 7 days yr^{-1} and unplanned downtime of 2–3 days yr^{-1}.

Table 2
Parameter values for the UK-based epoxy resin production facility.

Parameter	Symbol	Value	Units/Notes
Plant and Production Parameters			
Annual production capacity	P_{resin}	100 000	tonnes/year
Thermal energy intensity	$E_{\text{th,req}}$	0.8	MWh_{th}/tonne resin
Annual thermal energy demand	$E_{\text{th,total}}$	80 000	MWh_{th}/year (avg. ≈ 9.13 MW)
Sequestrable emissions	E_{nese}	8 000	tonnes CO2/year
Non-sequestrable emissions	E_{nense}	2 000	tonnes CO2/year
CHP System and Energy Balances			
Fraction for electricity	ρ_{energy}	0.25	–
Fraction for heat	$1-\rho_{\text{energy}}$	0.75	–
Installed CHP capacity	C_{CHP}	12	MW (thermal + electrical)
Ramp-up and ramp-down rates	R_{up}, R_{down}	1	MW/h
Heat Storage Parameters			
Maximum storage capacity	$Q_{\text{max,storage}}$	20	MWh
Storage (charging) efficiency	η_{storage}	0.90	–
Withdrawal efficiency	$\eta_{\text{withdrawal}}$	0.95	–
Decay factor (storage losses)	λ	0.99	per hour
Operational Flexibility and Ancillary Services			
Ancillary reduction cap	ϕ_{flex}	0.12	Fraction of baseline load (variable on investment)
Efficiency Parameters			
Thermal efficiency base constant	$\alpha_{\text{therm,NG}}$	0.60	–
Thermal efficiency load constant	$\beta_{\text{therm,NG}}$	0.002	per MWh
Thermal efficiency temp. constant	$\gamma_{\text{therm,NG}}$	−0.0002	per °C
Electrical efficiency base constant	$\alpha_{\text{elec,NG}}$	0.30	–
Electrical efficiency load constant	$\beta_{\text{elec,NG}}$	0.001	per MWh
Electrical efficiency temp. constant	$\gamma_{\text{elec,NG}}$	−0.0001	per °C
Production			
Production conversion factor	ψ	1.25	tonnes/MWh_{th}
Approx margin	P_{resin}	1000	$/tonne resin
Exogenous Annual Demand Parameters			
Annual electricity demand	$E_{\text{elec,total}}$	20 000	MWh/year (avg. ≈ 2.28 MW)
Annual refrigeration demand	$E_{\text{ref,total}}$	5 000	MWh/year (avg. ≈ 0.57 MW)
Electrical cooling COP	COP_e	3	–
Absorption cooling COP	COP_h	2	–

- **On-Site CHP Unit:** A ten-year-old combined heat and power system meets a portion of both thermal and electrical demand, hence its thermal efficiency is slightly less than that of new equivalents.

In this framework, demands for process utilities — thermal energy, electricity and refrigeration — are treated as exogenous inputs used to compute fuel burn, production throughput and CO_2 emissions. For the case study, we assume a fixed (stationary) utility-demand profile over the planning horizon: demands vary within each year to reflect the site's typical operating pattern (e.g. seasonality and planned shutdowns), but the overall production scale is not assumed to trend upward or downward over time. This is a case-study specification rather than a structural limitation of the framework. If anticipated changes in throughput, product slate, or utilization are available, they can be represented through time-varying demand and availability parameters, which would propagate through to investment timing and capacity decisions. The full set of plant-specific parameters used to instantiate the case-study model is given in Table 2. Tables 3 and 4 summarize the inputs and justification used to generate the market data and events, respectively.

3.2. Model building

The optimization model was developed in Pyomo 6.9.4 using Gurobi 12.1 and implemented in Python 3.11 and solved on an Intel(R) Core(TM) i9-14900HX CPU [42,43]. Stage 1 has 13,159 variables (12,945 continuous; 214 binary) and 12,670 constraints (7091 equalities; 5579 inequalities) and is terminated at a relative MIP optimality gap of 1 %. In a representative scenario Stage 1 solves in approximately 36 s. Each annual Stage 2 subproblem has 245,294 variables (245,292 continuous; 2 binary) and 219,008 constraints (122,647 equalities; 96,361 inequalities) and solves in approximately 68 s on average; therefore, Stage 2 requires 30 annual solves per scenario, corresponding to ∼2040 s (≈34 min) cumulative dispatch time, and an end-to-end runtime of ∼2076 s (≈35 min) per scenario when combined with Stage 1.

4. Results

4.1. Introduction to simulations

To assess the robustness of our optimization framework and investment decisions, we run five distinct scenarios outlined in Table 5, that vary key market parameters (Appendix E, Table 10), policy settings, and operational assumptions. Each scenario uses correlated market inputs generated by the model, along with prescribed policy or infrastructure constraints, enabling comprehensive "what-if" analysis under jointly varying market conditions. Table 4 shows exogenous events, such as energy crisis, subsidies and breakthroughs which are applied across all scenarios.

Table 3
Key market inputs and correlation anchors (Base-case scenario for 2025 and 2055). 2025 prices are based and adjusted by the bulk purchasing power of the plant, and is defined as "large" as per [44]. Other market inputs are tabulated in Appendix E, Table 11.

Variable	Symbol	2025	2055	Notes/Source
Prices (real USD kWh^{-1})				
Electricity	$P_{elec}(t)$	0.22	0.06	1% yr^{-1} decline; EIA AEO 2023 [45].
Natural gas	$P_{ng}(t)$	0.045	0.034	Flat long-run view; IEA Gas Report 2025 [46].
Hydrogen (LHV)	$P_{h_2}(t)$	0.192	0.06	Falls to \$2 kg^{-1} by 2030; IEA *Future of H_2* [47].
Biogas	$P_{biom}(t)$	0.12	0.07	Moderate learning; IEA Bioenergy 2022 [48].
Carbon and emission factors				
Carbon-credit price (USD tCO_2^{-1})	$P_{CC}(t)$	80	150	EU ETS long-run industrial trajectory [49,50].
Free allowances[a] (t CO_2 yr^{-1})	C_{free}	37 000	0	−4.3% yr^{-1} constant (CBAM listed sectors).
Emission intensities (t CO_2 per unit)				
Grid CO_2 intensity	$\zeta_{elec}(t)$	0.28	0.05	80% renewables by 2035 [51].
NG CO_2 intensity	$\zeta_{ng}(t)$	0.20	0.18	LNG spike until 2030 [45].
H_2 CO_2 intensity	$\zeta_{h_2}(t)$	0.12	0	Grey → green shift [47].
Biomass CO_2 intensity	$\zeta_{biom}(t)$	0.01	0	Near-neutral lifecycle [48].
Correlation anchors				
Elec/H_2	ρ_{elec,h_2}	0.40	0.90	Grey→ green transition ties cost to electricity [47].
Elec/NG	$\rho_{elec,ng}$	0.80	0.40	Renewables decouple electricity from NG [52].
NG/Biomass	$\rho_{ng,biom}$	0.20	0.20	Distinct supply chains keep link weak [45].

[a] *We adopt a stylized, deliberately conservative free–allocation path for high-leakage chemical products: benchmark-based EU ETS allowances continue after 2035 and decline linearly to zero by 2050. This path is chosen to isolate technology and market fundamentals while accentuating allowance banking, investment timing, and hedging, to provide an upper-bound test of robustness to tighter policy regimes.* Directive (EU) 2023/959 links free allocation to CBAM for covered goods from 2026; many chemical products are not currently CBAM goods and future scope remains under assessment at time of writing.

Table 4
Exogenous market–disturbance scenarios. Multiplicative factors (×baseline) are applied to the indicated price series for the duration of each event.

Event	Start	End	Price factors applied
Energy Crisis	2029–10–01	2030-03-31	$P_{ng} \times 2.0,\ P_{elec} \times 2.5,\ P_{h_2} \times 2.5,\ P_{biom} \times 2.0$
CBAM Uptake	2030–01–01	2055-12-31	$P_{CC} \times 1.2$
Severe Winter Storm	2032–01–01	2032-01-31	$P_{elec} \times 1.15,\ P_{ng} \times 1.2$
Biomass Subsidies	2032–01–01	2055-12-31	$P_{biom} \times 0.9$
Supply-chain Disruption	2035–01–01	2035-12-31	$P_{biom} \times 1.25,\ P_{ng} \times 1.25$
H_2 Production Breakthrough	2035–01–01	2055-12-31	$P_{h_2} \times 0.9$
Heatwave	2045–07–01	2045-07-31	$P_{elec} \times 1.1$

Table 5
Definition of scenarios and sub-cases.

Scenario	Key assumptions/constraints	Main purpose/policy question
Base (Benchmark)		
	UK meets all 2030s decarbonization milestones; credit banking allowed; default ETS cap-tightening.	Sets an "ideal" case: how a rational plant decarbonizes under favorable market and policy conditions.
A: Infrastructure limitations		
A1	Electrical grid expansion is limited; only repurposed NG pipelines supply H_2; default carbon price.	How long can the plant defer action when fuels and allowances stay relatively cheap?
A2	Same physical limits as A1, but the carbon price is allowed to rise endogenously until the market clears.	What carbon price is needed to pull investment forward in an infrastructure-constrained world?
B: Delayed grid decarbonization		
B1	Grid (and therefore green H_2) remains carbon-intensive until 2050; carbon price unchanged.	"Do-nothing" least-cost benchmark under weak policy.
B2	Same grid delay as B1, but the carbon price rises.	Can a steeper price signal enable biomass to compensate for the slow power-sector transition?
C: No banking of credits		
	Annual reconciliation; allowances cannot be banked or borrowed.	Without inter-temporal arbitrage, is early abatement still optimal?
D: Forced CCS		
	Carbon price exogenously raised to \$305 t^{-1} CO_2; post-combustion CCS becomes least-cost.	At what (steep) price does CCS out-compete simpler fuel-switch options for this plant configuration?

Table 6
Master summary of key performance indicators across scenario groups.

KPI	Base	A		B		C	D
		A1	A2	B1	B2		
Investment CAPEX ($M)	6.67	5.47	5.9	0	0	6.45	14.3
Fuel Cost ($M)	276	233	278	202	290	261	286
Carbon Compliance Cost ($M)	29.8	88	84	144	131	47.3	−20.1
Total CO_2 Emissions (Ktons)	650	1025	810	1395	1012	761	387
Ancillary Profit[a] ($M)	7.1	0	0	0	0	6.6	0
Other Revenues[b] ($M)	1.82	2.31	2.57	2.82	1.68	1.94	0.3
Additional Costs ($M)	0	0	0	0	0	0	27
Investment Year	2035	2044	2039	N/A	N/A	2038	2031
Primary Fuel	E	H_2/NG	H_2	NG	NG/BM	E	NG-CCS
Total Cost ($M)	304	323	355	342	419	306	307

[a] Profit generated after any loss in production or shortfall.
[b] Revenue generated from selling excess heat and electricity.

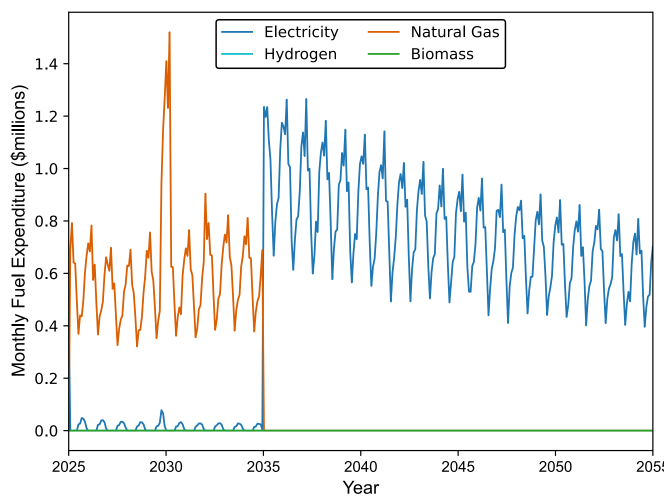

Fig. 2. Baseline Scenario: Monthly fuel expenditures (US$ millions) of electricity (blue), hydrogen (aqua), natural gas (orange) and biomass (green) from 2025–2055. After decarbonizing via electrification in 2035, all natural gas purchases are effectively converted into electricity purchases. (For interpretation of the references to color in this figure legend, the reader is referred to the web version of this article.)

4.2. Overview of all scenarios

Table 6 presents the headline quantitative outcomes for each case, listing the key performance indicators such CAPEX, fuel expenditure, carbon-compliance cost, cumulative CO_2, and so on. Monetary values are expressed in real 2025 USD; emission figures are in metric tonnes of CO_2 equivalent unless noted otherwise. The subsections that follow unpack these results in further depth.

4.3. Baseline scenario

We initially implement our model under a baseline scenario that assumes full attainment of all UK government targets. Although this assumption may be considered optimistic, it establishes an ideal benchmark for assessing our model's performance under favorable policy conditions.

Under this scenario, the model opts to invest in the electrification of heat production after ten years (in 2035). This investment aligns with the anticipated decarbonization of the UK electricity grid, ensuring that all purchased electricity for steam production from 2035 onward is low-carbon. Fig. 2 shows that fuel expenditure prior to 2035 consists of a mix of natural gas and electricity, whereas post-2035 it shifts entirely to electricity. Although electric boilers operate at approximately 98 % efficiency compared to an average of 76 % for the CHP system, more money is spent on purchased electricity to achieve the same heat output. This is also influenced by the assumed electricity price trajectory: the peak around 2030 is introduced via exogenous "energy crisis" modifiers (Table 4), while the gradual decrease in average electricity cost thereafter follows the baseline scenario assumptions (Table 3) and these patterns are observed across all fuel expenditure graphs. Even by 2055, the fuel cost remains higher than what would have been incurred with natural gas, only since it is more optimal to offset carbon compliance costs instead.

Fig. 3 provides an annual summary of carbon credit trading dynamics, where the plant is required to surrender credits equivalent to the previous year's emissions. Importantly, the quantity shown as "banked" is a year-end *stock* of accumulated credits carried forward (including balances from earlier years), whereas "earned" denotes the *flow* of surplus credits generated within that specific year. As a result, the year-end banked balance can exceed the credits earned in a given year because it reflects cumulative carryover over multiple years, not only the current-year surplus. This "early" decarbonization enables the plant to accumulate carbon credits over several years, which are sold once carbon prices peak and begin to stabilize around 2041. Despite the transition, the number of carbon credits that must be purchased increases annually due to residual non-energy system emissions and reducing free allocations.

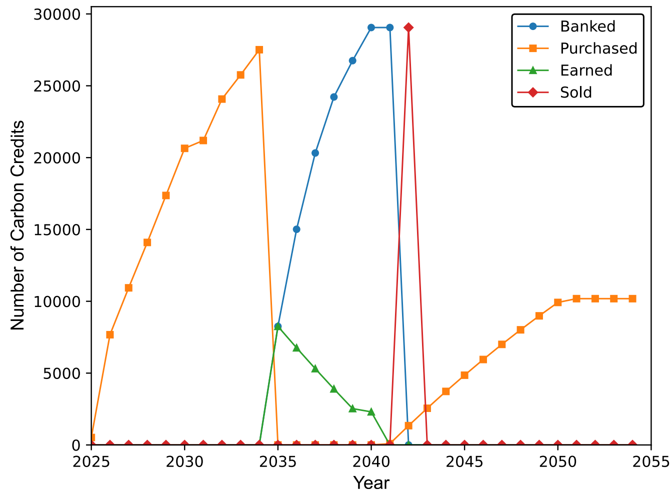

Fig. 3. Baseline Scenario: Carbon-credit dynamics(2025–2055). Annual credits (tCO_2) by category: banked—solid blue with circle markers; purchased—solid orange with square markers; earned—free allocations in excess of process emissions—solid green with triangle markers; sold—solid red with diamond markers. After plant decarbonization in 2035, allocations exceed emissions until 2040 and are therefore banked from 2035 onward.

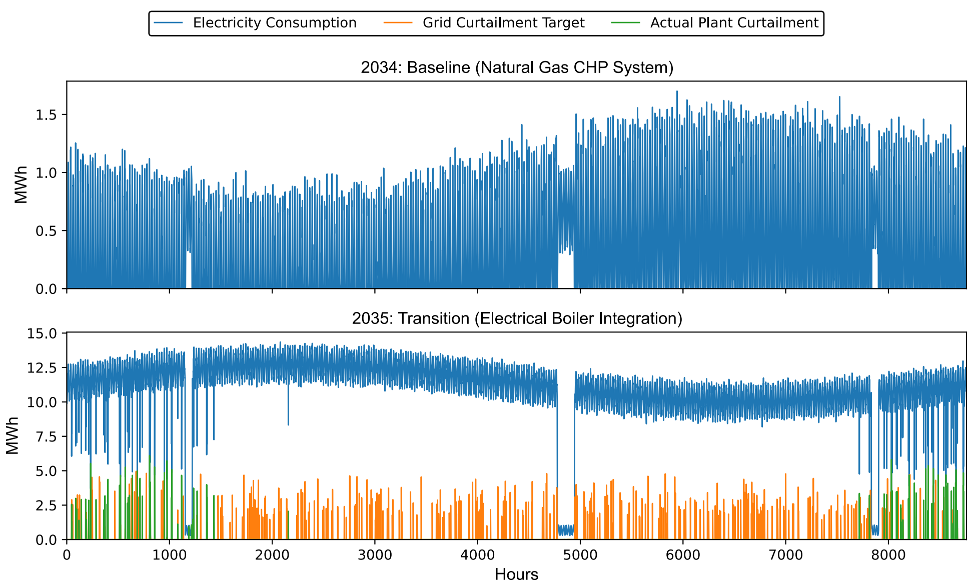

Fig. 4. Baseline Scenario: Hourly electricity consumption of the chemical plant depicted for two different years: before (top panel) in 2034 and after (bottom panel) the investment in an electric boiler in 2035. The blue line represents the plant's hourly consumption, the orange line indicates the grid's curtailment target, and the green line shows the actual curtailment achieved by the plant at each hour. (For interpretation of the references to color in this figure legend, the reader is referred to the web version of this article.)

Fig. 4 illustrates the effect of plant electrification on ancillary market participation by comparing electricity consumption profiles before and after the transition. The top panel shows the plant's hourly electricity consumption in 2034 (pre-investment), while the bottom panel displays the higher consumption in 2035 following the electric boiler investment, reflecting the plant's former heat load converted into electricity load, all of which is now procured from the grid. The plant only curtails load during the winter months when seasonal electricity prices narrow operating margins, making it advantageous to reduce production in exchange for ancillary revenue. However, the total revenue generated is approximately $7.21 million over the boiler's 20-year lifetime—an average of only about $0.36 million per year—which is insufficient to offset the higher electricity procurement costs incurred by investing earlier (in fact, the sooner the electrification is brought forward, the greater the cumulative fuel costs), resulting in a net shortfall against the increased OPEX. This ancillary revenue corresponds to a life-time cost reduction of less than 4 %, indicating that it has virtually no effect on the investment decision or its timing. In this case, the high profit margin of the manufactured commodity favors maintaining a high production rate; conversely, if the margin were significantly lower, ancillary market participation could have more influence on the investment strategy.

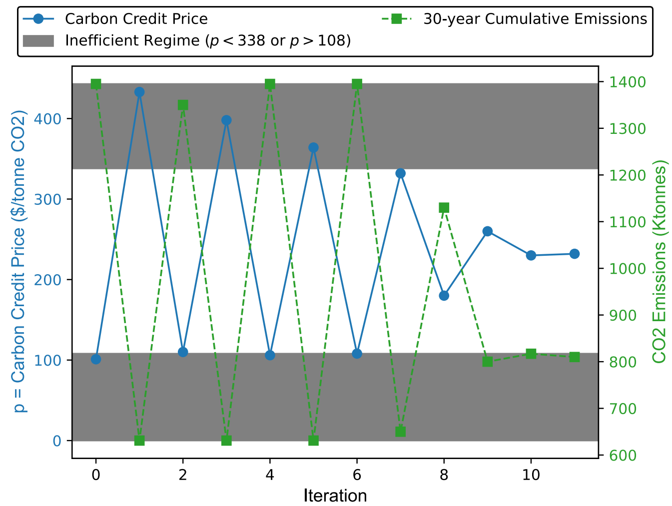

Fig. 5. Scenario A2: Carbon-credit price iteration and abatement response (2025–2055). Left axis: carbon price p (US\$ tCO_2^{-1}); right axis: 30-year cumulative emissions (kt CO_2). Carbon price—solid blue with circle markers; emissions—dashed green with square markers. Gray bands denote the "inefficient" region where p lies outside the target corridor [108, 338] US\$ tCO_2^{-1} where further price changes induce no abatement response. The sequence converges to an equilibrium near $p \approx 230$ US\$ tCO_2^{-1}.

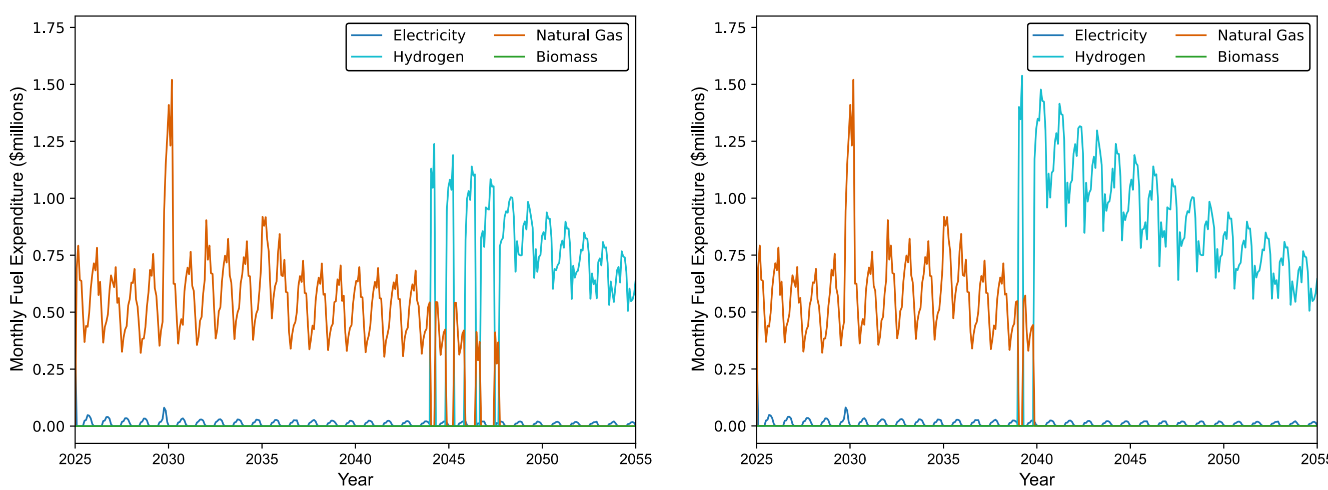

(a) (b)

Fig. 6. Scenario A: Monthly fuel expenditures (US\$ millions) of electricity (blue), hydrogen (aqua), natural gas (orange) and biomass (green) from 2025–2055. Panel (a): scenario A1; panel (b): scenario A2. In scenario A1, natural gas purchases are converted into hydrogen in 2044 after decarbonizing, with a mixture of both until 2048. In scenario A2, investment is instead made in 2039 driven by a higher carbon price. (For interpretation of the references to color in this figure legend, the reader is referred to the web version of this article.)

4.4. *Scenario A: Infrastructure limitations*

This scenario investigates the decarbonization pathway under constrained infrastructure conditions. Hydrogen infrastructure is assumed to be available via the repurposing of existing natural gas pipelines, while additional electricity transmission capacity remains limited due to regulatory and policy-induced delays.

In case A1, the plant retrofits its CHP system to hydrogen in 2047. However, full decarbonization is deferred until 2050, as the plant uses both hydrogen and natural gas to exploit seasonal fuel price variations, shown in Fig. 6. This delayed transition reflects the limited competitiveness of hydrogen and carbon pricing under current government targets, resulting in increased lifetime CO_2 emissions. This results in a \$50M increase in carbon compliance costs relative to the base case; however, this is partially offset by the lower cost of natural gas, reducing the fuel cost by \$18M, but overall emissions are 70 % higher.

In case A2, to encourage an earlier investment and reduce life-time emissions, we search for a carbon price that can induce faster emissions reductions if no plants decided are able to decarbonize due to the lack of electricity infrastructure to assess how this might impact the overall carbon market. High emissions trigger an increase in carbon credit demand, driving the price upward from an initial \$150 per tonne CO_2 to an equilibrium level of approximately \$230 per tonne CO_2 (see Fig. 5). Under this new carbon price, the plant decides to retrofit its CHP system to hydrogen in 2038 instead, 9 years earlier, achieving a 26 % reduction in lifetime emissions relative to Case A1. This improvement, however, comes at a cost: overall fuel expenditures increase by \$49M and total system costs by \$32M, indicating that reliance on carbon pricing alone is insufficient

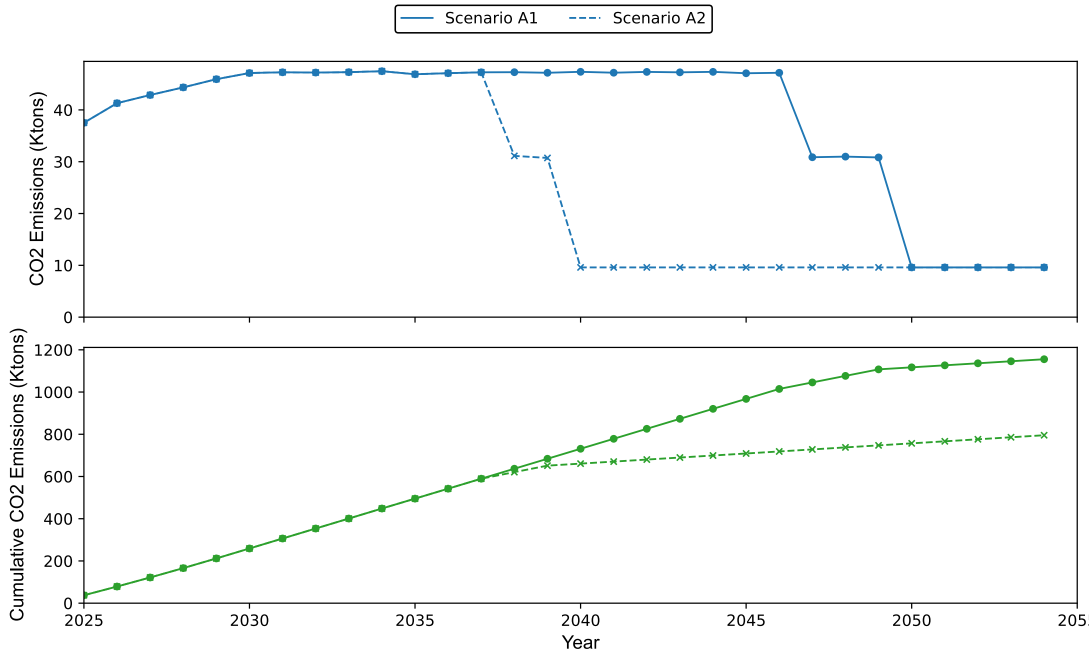

Fig. 7. Scenario A: Annual and cumulative CO_2 emissions for scenarios A1 and A2 (2025–2055). Top panel: annual emissions (kt CO_2 yr^{-1}). Bottom panel: cumulative emissions from 2025 (kt CO_2). Scenario A1—solid lines; A2—dotted lines. Annual emissions drop significantly after investment is made in 2039 in A2, resulting in cumulative emissions curving off, but in A1 this drop is much later in 2048, resulting in significantly greater cumulative emissions.

for an optimal transition, leading to inefficient cost increases, and that complementary measures—such as electrification or competitively priced hydrogen and biomass—are necessary. In reality, an inefficient carbon market would trigger the introduction of additional policy safeguards, to prevent carbon prices from spiraling to unrealistic levels.

Fig. 7 presents the cumulative CO_2 emissions from 2025 to 2055, illustrating the environmental and economic implications of the delayed transition in Case A1.

4.5. Scenario B: Delayed grid decarbonization

In this scenario, we assume that the UK fails to meet its 2035 grid decarbonization target, with full decarbonization occurring only by 2050. Consequently, green electricity remains largely unavailable in the near term, constraining the supply of green hydrogen. Under unchanged carbon policy settings, these limitations drive up the costs of both fuels, forcing the plant to rely on fossil fuels while incurring substantial carbon compliance expenses.

In Case B1, no new investments are made. With the grid remaining carbon-intensive until 2050, it becomes uneconomical for the plant to invest in any decarbonization technology. Natural gas remains the most competitive fuel option, resulting in the lowest overall fuel costs among all scenarios; however, this comes at the expense of a significant compliance cost of \$144M. Over a 30-year horizon, not decarbonizing incurs an additional cost of \$52M compared to the base case, which, for a plant of this size, is a relatively modest penalty for a risk-neutral strategy, though more stringent policies or market pressures would likely force decarbonization in other ways.

In Case B2, we assume the carbon market reacts to plants lacking the ability to decarbonize and search for an equilibrium price. Under these conditions, the model begins to incorporate biomass into the fuel mix at carbon prices above \$205/tonne CO2 (see Fig. 8). Moreover, since biomass can be readily blended into existing systems without new capital expenditures, the plant retains the flexibility to revert to natural gas if necessary, rendering the biomass option effectively risk-free in the face of price volatility.

In practice, if the ETS fails to drive decarbonization effectively, additional policy interventions, such as targeted subsidies for hydrogen or biomass integration, or adjustments to the cap tightening schedule, would likely be necessary to achieve similar outcomes to the base-case scenario. If these base-case targets are not achieved such as in this scenario, producers would most likely not be forced to decarbonize, and instead, regulatory frameworks might favor a less stringent cap tightening regime with the increased provision of free allowances to accommodate the delay in grid decarbonization until the option becomes viable (see Fig. 9).

4.6. Scenario C: No banking of credits

In this scenario, the plant is not permitted to hold, aka, ‘bank’ carbon credits across multiple years, reflecting certain emissions trading systems that enforce annual reconciliation (e.g., South Korea), or plants that want to avoid any arbitrage uncertainty. There is little incentive to decarbonize earlier than strictly necessary to meet immediate compliance. As a result, the electrification investment in Scenario C is delayed by approximately three years relative to the baseline (investing in 2038 instead of 2035), and overall project emissions rise.

Fig. 10 illustrates the plant’s carbon credit dynamics under this no-banking rule. In every year, any earned credits are sold immediately, producing short-term revenue but eliminating any arbitrage possibilities. In principle, one might expect forced liquidation of credits to induce market volatility, as allowance prices fluctuate more acutely in response to annual supply–demand imbalances. From the plant’s perspective,

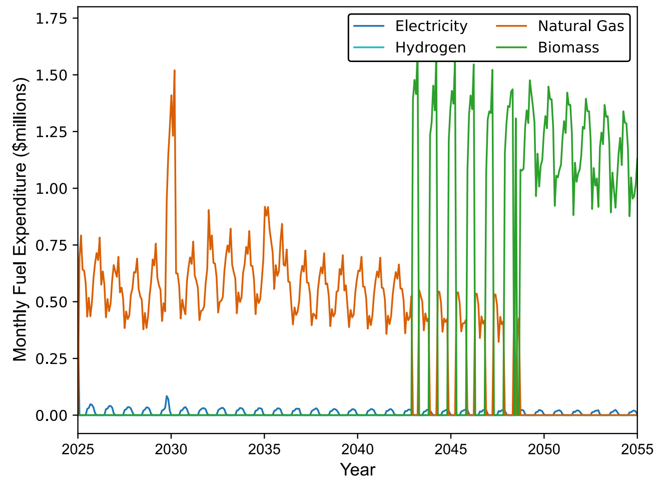

Fig. 8. Scenario B2: Monthly fuel expenditures (US$ millions) of electricity (blue), hydrogen (aqua), natural gas (orange) and biomass (green) from 2025–2055. Extremely high carbon prices and the limitation of other decarbonization routes enable biomass as a viable fuel-switching option. (For interpretation of the references to color in this figure legend, the reader is referred to the web version of this article.)

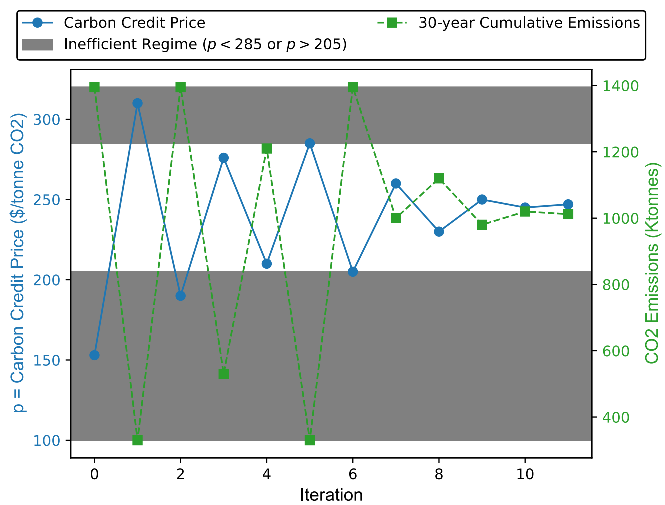

Fig. 9. Scenario B2: Carbon-credit price iteration and abatement response (2025–2055). Left axis: carbon price p (US$ tCO_2^{-1}); right axis: 30-year cumulative emissions (kt CO_2). Carbon price—solid blue with circle markers; emissions—dashed green with square markers. Gray bands denote the "inefficient" region where p lies outside the target corridor [205, 285] US$ tCO_2^{-1} where further price changes induce no abatement response. The sequence converges to an equilibrium near $p \approx 253$ US$ tCO_2^{-1}.

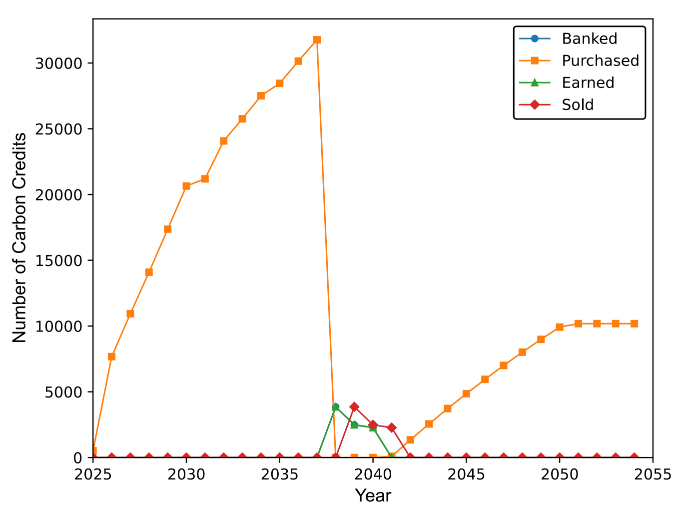

Fig. 10. Scenario C: Carbon-credit dynamics (2025–2055). Annual credits (tCO_2) by category: banked—solid blue with circle markers; purchased—solid orange with square markers; earned—free allocations in excess of process emissions—solid green with triangle markers; sold—solid red with diamond markers. After plant decarbonization in 2038, all earned credits are immediately sold the following year.

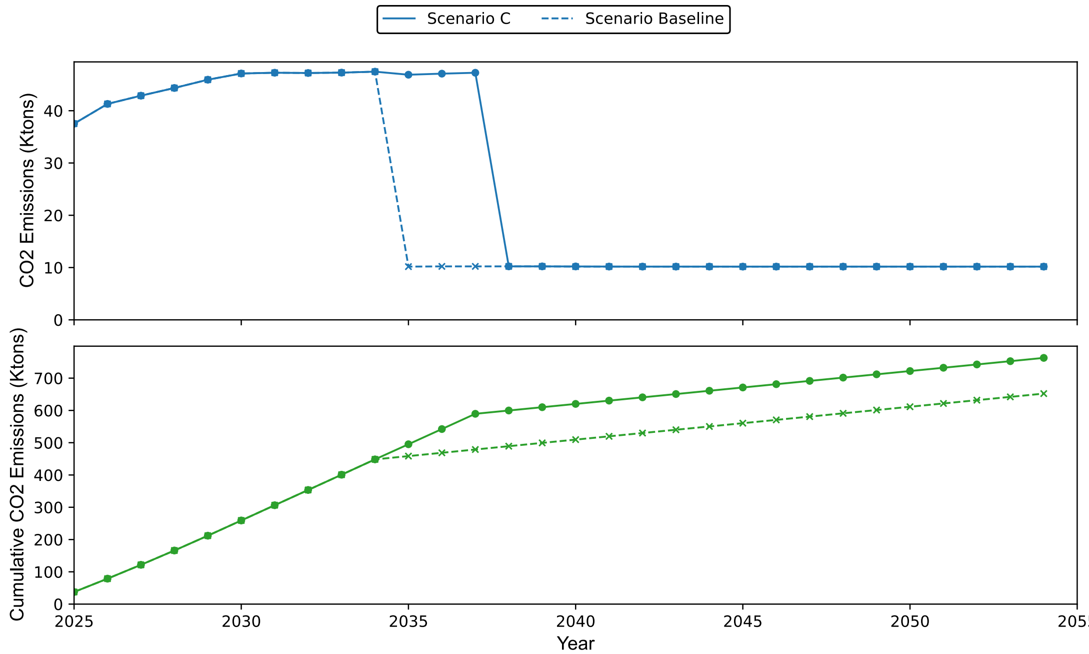

Fig. 11. Scenario C: Annual and cumulative CO_2 emissions for scenarios C compared to the baseline scenario (2025–2055). Top panel: annual emissions (ky $CO_2\,yr^{-1}$). Bottom panel: cumulative emissions from 2025 (kt CO_2). Scenario C—solid line; Baseline—dotted line. The ability to bank gives a more efficient time-dependent cost-emissions trade-off enabling earlier investment in the baseline scenario compared to C.

however, short-run compliance costs do not motivate early abatement when there is no prospect of holding (and potentially profiting from) surplus credits in future, higher-priced markets, removing any cost/emissions tradeoff.

Despite the delay, the total life-cycle cost to the plant remains effectively unchanged compared to the baseline. Fig. 11 shows that the main consequence is a net increase in cumulative emissions of about 110 kton CO_2. Since the cost impact is negligible, the plant experiences no meaningful penalty for delaying decarbonization. In policy terms, this indicates an inefficiency: although the company avoids significant additional financial risk, the scenario effectively shifts emissions into later years rather than reducing them overall, ultimately producing higher lifetime CO_2 emissions. Moreover, by removing the possibility of holding credits as a hedge or strategic asset, the policy could introduce heightened volatility into the carbon market, since large emitters all offload allowances at once each period.

4.7. Scenario D: Forced CCS

In this scenario, the carbon price is increased until CCS system becomes the preferred pathway. A carbon price of \$305 / t CO_2 is required for CCS to match the baseline scenario's net present cost.

CCS is implemented in 2031. Once operational, the system captures about 92 % of the plant's residual emissions—those not already abated through further electrification or low-carbon fuels.

The model opts for an auxiliary electric boiler rather than expand on-site fuel combustion. The associated energy penalty is around 2 MWh per tonne of CO_2 captured, driving electricity consumption and costs sharply upward post-2030. Fig. 12 shows how captured CO_2 credits accumulate to nearly 130 kt, whereas Fig. 13 depicts the increase in electricity expenditure. Transport, storage, and amine-regeneration requirements add approximately \$27 million.

For this particular plant, a large fraction of total emissions can be mitigated by modifying the energy system, leaving relatively few *residual* emissions for CCS to target—making the technology economically viable only at an unrealistically high carbon price. In contrast, plants with higher shares of *uncapturable* emissions (e.g., process CO_2 streams that cannot be readily abated by fuel switching) may find CCS profitable at lower carbon prices. Thus, although our scenario suggests that CCS is uneconomical under most moderate-pricing policies, this conclusion primarily reflects the extent to which simpler decarbonization strategies can already reduce emissions at this specific site. Under different industrial configurations or more carbon-intensive processes, CCS could become competitive at lower carbon prices.

5. Discussion

5.1. Technology maturity and plant-level feasibility

The model assumes that low-carbon technologies and the requisite infrastructure are available; in practice, deployment is constrained by technology maturity, site integration, and permitting and supply-chain readiness.

Electrification is currently most mature for medium-temperature steam services (roughly 350–400 °C at moderate-to-high pressures), whereas many high-temperature processes (e.g., steam cracking >500 °C) remain beyond commercially viable. High-temperature electric furnaces and

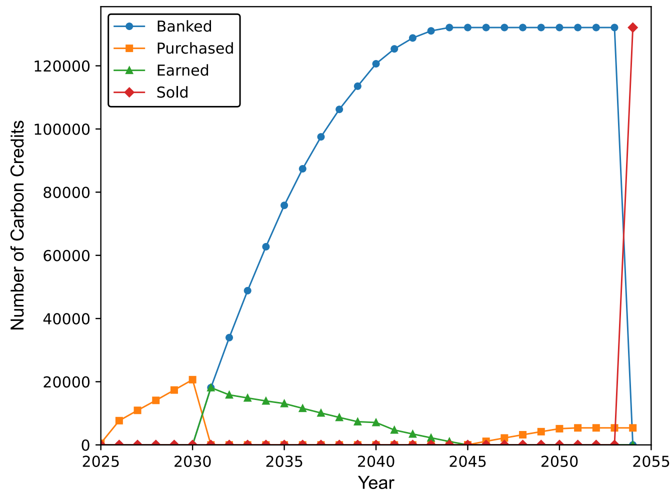

Fig. 12. Scenario D: Carbon-credit dynamics (2025–2055). Annual credits (tCO_2) by category: banked—solid blue with circle markers; purchased—solid orange with square markers; earned—free allocations in excess of process emissions—solid green with triangle markers; sold—solid red with diamond markers. After investment in CCS in 2031, a large amount of credits are earned, and are banked until the value of carbon credits in this scenario rises to $305 / $t\,CO_2$), and peaks at the end of the investment horizon.

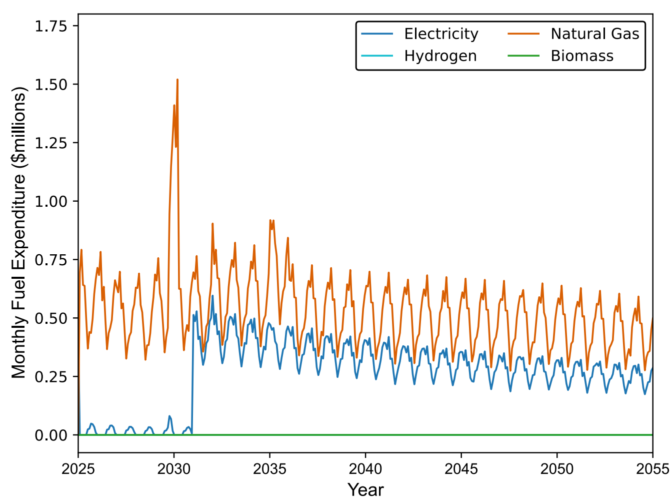

Fig. 13. Scenario D: Monthly fuel expenditures (US$ millions) of electricity (blue), hydrogen (aqua), natural gas (orange) and biomass (green) from 2025–2055. Investment in CCS in 2031 substantially increases electricity demand due to auxiliary electric boilers for thermal regeneration of solvent. (For interpretation of the references to color in this figure legend, the reader is referred to the web version of this article.)

burners are under active development, but their cost and performance trajectories remain uncertain, and premature deployment can introduce lock-in risk. Consistent with this, electrification is selected in the baseline scenario but becomes infeasible in Scenario A, where electrification is disallowed; total decarbonization costs increase substantially, illustrating that electrification's competitiveness is strongly case-dependent and constrained by process temperature requirements.

Hydrogen combustion provides broader temperature coverage (up to and beyond 1000 °C) and can often be retrofitted into existing burner systems with less disruption than full equipment replacement. Although hydrogen pathways can be more expensive in operating cost than electrification under many price trajectories, they offer operational flexibility and can provide a pragmatic transition option where electrification is technically constrained or where fuel switching is desired without extensive process redesign.

5.2. Policy credibility and imperfect foresight

The case study highlights that least-cost decarbonization pathways can be sensitive to long-run policy and system assumptions that are outside the control of the plant. In the base case, we assume the UK grid's carbon intensity falls below $50\,g\,CO_2\,kWh^{-1}$ by 2035, under which full electrification of steam emerges as the lowest-cost option. When this trajectory is relaxed, for example if grid intensity remains above $100\,\mathrm{g\,CO_2\,kWh^{-1}}$ until 2040, the model reverts towards BAU operation. This illustrates the opportunity cost and regulatory risk of anchoring long-lived investment decisions to optimistic decarbonization timelines.

A second realism consideration is the perfect-foresight structure implicit in each deterministic scenario. Under perfect foresight, the optimizer can time investments exactly when assumed policy thresholds are reached and when relative prices switch, which understates frictions faced by industrial decision-makers. The formulation therefore abstracts from multi-year supply and off-take contracting constraints, permitting and financing lead times, and discrete planning cycles that typically limit how precisely investments can be synchronized with evolving policy milestones. Results should be interpreted as cost-effective target pathways conditional on each scenario, rather than as an implementable year-by-year investment plan.

A related computational consideration is the two-stage structure adopted to manage scale. In the present implementation, Stage 1 determines investment timing and capacity expansion on an aggregated time grid, while Stage 2 optimizes hourly operation to quantify feasibility, operating costs and revenues, and short-timescale value streams (e.g. demand response or load shedding). However, Stage 2 outcomes do not feed back to revise Stage 1 investment decisions. Consequently, the resulting investment pathway is not guaranteed to coincide with the fully integrated hourly investment–dispatch optimum; in particular, the model may understate the long-run value of operational flexibility and may miss investment choices whose attractiveness is driven primarily by short-duration price extremes or ancillary-market revenues.

Both perfect foresight and single-scenario specialization motivate uncertainty-aware extensions. Stochastic or robust formulations can select strategies that perform well across multiple plausible market–policy realizations and explicitly value recourse, i.e., the ability to adapt investments and operations as uncertainty resolves. A practical implementation is rolling re-optimization, in which investment decisions are periodically updated as information on prices, policy milestones, and technology costs changes, while respecting sunk investments and commissioning lead times. In addition, real-world delivery typically depends on complementary market arrangements and policy instruments that reduce revenue and cost uncertainty, such as longer-term off-take and hedging arrangements (e.g. fixed-price supply contracts or collars) and carbon-policy designs that provide clearer forward guidance (e.g. price corridors or tighter commitment to milestone delivery).

5.3. Price volatility and risk-buffer mechanisms

Carbon pricing acts as a “buffer” that determines how large a premium a plant can tolerate for low-carbon energy carriers relative to natural gas. In Scenario A1, hydrogen is adopted only late in the horizon (2047) because early-period delivered costs remain above what the prevailing carbon-price path can justify. This indicates that, under the trajectories considered, earlier switching requires risk-reduction mechanisms that lower the effective premium faced by the plant, such as long-term fuel-price guarantees or hedging structures (e.g. fixed-price contracts, forwards, or collars) that smooth delivered costs over time.

Scenario A2 increases carbon prices to induce earlier switching and shows that the required price level exceeds approximately $\$200\,\mathrm{tCO_2^{-1}}$. This is well above typical policy expectations and suggests that carbon pricing alone is unlikely to bridge sustained green-fuel premia under plausible cost trajectories. Volatility in hydrogen and electricity prices further weakens the buffer: short-lived spikes can make low-carbon operation temporarily unattractive and increase downside exposure. These results motivate complementary instruments that address both uncertainty and volatility. For example, Dynamic Adaptive Policy Pathways (DAPP) approaches can define decision points and “signposts” at which pre-agreed adjustments (e.g. corridor tightening or activation of price guarantees) are triggered when observed conditions deviate from expectations.

5.4. Permit banking as a strategic hedge

Scenario C quantifies the economic value of intertemporal arbitrage when banking of CO_2 allowances is permitted. Between 2035 and 2041 the model over-complies, accumulating $30\,\mathrm{kt\,CO_2}$ of credits that are sold at $\$153\,\mathrm{t^{-1}\,CO_2}$. Without banking, the solution lies on a stricter cost–emissions frontier; investment timing is then driven primarily by CAPEX learning and fuel-price trends, and lifetime emissions increase by $110\,\mathrm{kt\,CO_2}$ with a total-cost change of less than 1 %. While firms could, in principle, bank allowances strategically, hoarding incentives are constrained in practice by reserve mechanisms such as the MSR.

Banking has a particularly strong effect for CCS. With banking (Scenario D) the model captures 92 % of residual emissions and stores $130\,\mathrm{kt\,CO_2}$; if banking is disallowed, the additional operating cost outweighs the implied value and CCS is not deployed. The sensitivity of outcomes to banked volumes also highlights risk exposure: strategies that rely heavily on stored credits are more vulnerable to future rule changes and spot-price swings. Where banking materially contributes to value, complementary hedges (e.g. long-dated forwards or swaps) can stabilize cash flows while preserving incentives for early abatement.

As an illustrative example, a long-dated fixed-price swap (structured as a strip of forwards) starting in 2035 at a fixed $\$110\,\mathrm{t^{-1}\,CO_2}$ reproduces the baseline outcome without physical carry-over, replacing banking value with a contractual hedge. In practice, such a hedge would embed a risk premium and would require careful design to avoid reintroducing incentive distortions.

5.5. Biomass and carbon offsets

Across the scenario set, biomass alone is not cost-optimal unless carbon prices exceed approximately $\$250\,\mathrm{t^{-1}\,CO_2}$ (Case B2) and competing low-carbon fuel options are unavailable; under these conditions, biomass feedstock costs account for more than 80 % of total utility OPEX. Similarly, standalone CCS requires an ETS price near $\$305\,\mathrm{t^{-1}\,CO_2}$ (Scenario D) before capture becomes economically attractive given energy penalties and operating costs. Both thresholds exceed typical policy expectations.

These break-even prices reflect avoidance-only incentives. If policy provides a removal premium for each tonne of CO_2 permanently sequestered, the effective threshold can fall materially. For example, a removal certificate priced roughly $\$150\,\mathrm{t^{-1}\,CO_2}$ above avoidance credits would reduce the required ETS price for BECCS to approximately $\$150$–$\$155\,\mathrm{t^{-1}\,CO_2}$, bringing it closer to plausible policy levels once removals value is recognized.

Current UK-ETS treatment zero-rates sustainable biomass at the stack but does not grant a tradable removal unit; the operator primarily avoids purchasing allowances [53]. The UK green-house gas removals consultation proposes ex-post negative-emission certificates priced via long-term contracts, providing policy-stable revenue but unbankable within the ETS [54]. The draft EU CRCF aims to certify permanent-storage removals and proposes potential links to compliance use [55]. In voluntary markets, permanent-storage units can trade at multiples of avoidance prices [56]. Overall, credible removals policy with clear eligibility and value signals is a prerequisite for biomass and BECCS to move beyond niche deployment under the assumptions considered.

6. Concluding remarks and recommendations

We developed a policy-integrated planning–operations framework that combines multi-decadal investment timing with hourly dispatch evaluation under an explicit emissions trading system with intertemporal banking. By linking long-run capacity choices, hour-level operating outcomes, and allowance-market decisions, the framework shows how policy timing and market volatility can reshape least-cost decarbonization outcomes across a diverse range of future scenarios.

Across the scenarios evaluated, four insights emerge:

1. A synchronized grid decarbonization trajectory is critical. Electrification outperforms alternative routes only when grid carbon intensity falls below $50\,\mathrm{g\,CO_2\,kWh^{-1}}$ by 2035. Slower grid decarbonization shifts the optimum toward business-as-usual, generating an additional 745 kt of CO_2 emissions over 30 years.
2. Carbon pricing requires complementary risk-reduction mechanisms. A predictable floor can encourage earlier investment, yet even a $200 t^{-1} CO_2 price does not fully offset delivered green-fuel costs in the scenarios considered. Complementary instruments such as longer-term fuel-price guarantees (e.g., PPAs, fixed-price supply contracts, or hedging arrangements) are therefore important to reduce exposure to volatility and support earlier adoption.
3. Allowance banking reduces cost and can enable earlier abatement. Allowing intertemporal trading enables additional abatement in the base case (110 kt CO_2) by valuing early action and flexibility across compliance periods. Removing banking flattens the cost–emissions frontier and reduces flexibility.
4. CCS and biomass are niche options under the assumptions considered unless supported by additional value streams. Forced early CCS increases total cost by 30 %–40 %, while biomass without explicit recognition of removals value is not selected across the scenarios evaluated. Policies that credibly value removals and/or provide access to low-cost clean power are therefore important if these options are to play a larger role.

A central finding is the degree to which the preferred decarbonization strategy and its timing depend on the assumed future. The optimal pathway shifts markedly across scenarios, driven by changes in grid decarbonization timing, volatility in hydrogen and biomass costs, and alternative carbon-price trajectories. The framework therefore functions as a transparent stress-testing tool that can be rerun under alternative policy road-maps and technology outlooks to identify where policy credibility and timing are most consequential.

By tailoring investments and operating outcomes to a facility's characteristics, the model produces decisions that reflect operational constraints and economic trade-offs. Nonetheless, the framework should be tested on additional case studies spanning different industries and process configurations to examine how factors such as feedstock availability, process-utility demands, and local policy design vary across sites. Such cross-industry analysis would also help assess whether current policy designs inadvertently advantage certain sectors and would support more technology-neutral regulation design.

The analysis uses deterministic, perfect-foresight optimization within each scenario. In addition, the two-stage structure used for tractability means that hourly operational outcomes do not feed back to revise long-horizon investment timing decisions. Consequently, reported arbitrage values and investment timings should be interpreted as conditional on the assumed trajectory and are not guaranteed to match the fully integrated hourly investment–dispatch optimum. In practice, decision-makers face uncertainty about policy evolution, supply-chain bottlenecks, and technology learning rates, and cannot synchronize investments precisely to threshold-crossing events or market peaks. A natural next step is therefore to extend the framework toward decision-making under uncertainty using stochastic or robust optimization and rolling re-optimization. This would enable strategies that are less specialized to any single assumed future and explicitly value recourse, namely the ability to adapt investments and operations as uncertainty resolves.

Several limitations also motivate directions for future research. First, the case study uses a fixed operating profile and fixed production outputs over the 30-year horizon, but no long-run changes in throughput or product slate are imposed exogenously). In practice, industrial sites experience shifts in utilization and product mix driven by market demand and relative product prices. Extending the framework to incorporate time-varying production plans and, where relevant, to co-optimize production capacity alongside utility investments would improve realism. Second, we assume the required enabling infrastructure is available (e.g., hydrogen transport, biomass supply chains, and CO_2 transport and storage). Coupling the plant-level model to regional infrastructure deployment models would help capture rollout constraints, lead times, and sequencing effects. Finally, the present demonstration focuses on an epoxy-resin plant; applying the approach to other energy-intensive sectors (e.g., steel, cement, refining) would test transferability and clarify which levers and policy sensitivities are sector-specific.

Overall, the results indicate that technology readiness, price stability, and credible policy design must advance together. Risk mitigation requires transparent pathways, periodic reassessment, and practical instruments that reduce exposure to adverse outcomes. Carbon-price corridors, fuel-price guarantees, and supportive contracting structures can complement long-lived investment decisions, while recourse-based extensions can support least-regret strategies across uncertain futures. The framework presented here provides a scalable template for analyzing integrated policy–technology packages and guiding plant-level investment planning under evolving market and policy conditions.

7. Nomenclature

Symbol	Description	Units
Indices & Sets		
$h \in \mathcal{H}$	Hour index and set of hourly operating periods (Stage 2)	–
$m \in \mathcal{M}$	Month index and set of monthly planning periods (Stage 1)	–
$y \in \mathcal{Y}$	Year index and set of years	–
$t \in \mathcal{T}$	Technology index and set of candidate technologies (e.g., CHP, boiler, CCS)	–
$f \in \mathcal{F}$	Fuel index and set of fuels (e.g., natural gas, hydrogen, biomass)	–
$c \in \mathcal{C}$	Commodity index and set of commodities (e.g., electricity, gas, hydrogen, biomass)	–
$i \in \mathcal{I}$	Carbon-compliance interval index and set of compliance intervals	–
$j \in \mathcal{I}$	Allowance-disposal interval index (same universe as $\mathcal{I}$)	–
Capacity & Investment Variables		
$\overline{C}_t$	Maximum (design) capacity of technology t if installed (single-event case)	MW
$C_{\text{installed}}(t)$	Nominal capacity added per purchase unit of technology t (multi-stage case)	MW
$R_{\max}$	System-wide upper limit on total installed nominal capacities	MW
$A_{\text{tech}}(m,t)$	Cumulative installed units/capacity-availability indicator for technology t by month m (multi-stage)	– or MW
$I_{\text{tech}}(t)$	Total number of purchased units (or cumulative purchases) of technology t over horizon	–
$O_{\text{tech}}(m,t)$	Operational output/utilized capacity of technology t in month m (multi-stage)	MW
$x_{\text{purchase}}(m,t)$	Binary/integer: purchase decision for technology t in month m (multi-stage)	–
$x_{\text{invest},t}(m)$	Binary: 1 if single-event investment in technology t occurs in month m	–
$x_{\text{invest},t}$	Binary: 1 if single-event investment in technology t occurs at any time	–
$x_{\text{active},t}(m)$	Binary: 1 if technology t is active by month m (single-event activation)	–
$O_t(m)$	Operational output of technology t in month m (single-event formulation)	MW
$O_{\text{baseline}}(h)$	Available baseline (existing) steam capacity at hour h	MW_{th}
$O_{\text{boiler}}(h)$	Available auxiliary boiler steam capacity at hour h	MW_{th}
$P_{\text{purchase,boil}}(m)$	Additional boiler capacity purchased in month m (e.g., to supply CCS steam)	MW_{th}
$A_{\text{boiler}}(m)$	Cumulative installed auxiliary boiler capacity by month m	MW_{th}
Heat-Related Variables		
$Q_{\text{prod}}(h)$	On-site thermal (steam) production at hour h	MW_{th}
$Q_{\text{useful}}(h)$	Useful heat delivered to process demands at hour h	MW_{th}
$D_{\text{heat}}(h)$	Exogenous thermal demand at hour h	MW_{th}
$Q_t(h)$	Heat duty served by additional unit/technology t at hour h	MW_{th}
$Q_{\text{elec}}(h)$	Heat produced electrically at hour h (e.g., electric boiler)	MW_{th}

$Q_{\text{over}}(h)$	Surplus (waste/exportable) heat at hour h	MW_{th}
Thermal Storage		
$Q_{\text{stored}}(h)$	Stored thermal energy at end of hour h	MWh_{th}
$Q_{\text{withdrawn}}(h)$	Heat withdrawn from storage during hour h	MW_{th}
η_{storage}	Storage charging efficiency	–
$\eta_{\text{withdrawal}}$	Storage discharging efficiency	–
λ	Per-hour storage decay/retention factor (losses)	–
$Q_{\text{max,storage}}$	Maximum thermal storage energy capacity	MWh_{th}
Cooling & Refrigeration		
$Q_{\text{cooling}}(h)$	Cooling load served via absorption/thermal cooling pathway in hour h	MW_{th}
$\Delta H_{\text{cooling}}(h)$	Thermal energy input to absorption cooling in hour h	MW_{th}
COP_h	Coefficient of performance for thermal (absorption) cooling	–
$E_{\text{cooling}}(h)$	Electrical input to electric chiller in hour h	MW_e
COP_e	Coefficient of performance for electrical cooling	–
$R_{\text{prod}}(h)$	Total cooling production (electric + absorption) at hour h	MW_{th}
$D_{\text{refrigeration}}(h)$	Exogenous refrigeration/cooling demand at hour h	MW_{th}
Electricity-Related Variables		
$E_{\text{plant}}(h)$	On-site electrical generation delivered to plant loads at hour h	MW_e
$E_{\text{production}}(h)$	Gross electrical production by CHP at hour h	MW_e
$E_{\text{purchased}}(h)$	Electricity purchased from grid at hour h	MW_e
$E_{\text{useful}}(h)$	Useful electrical consumption at hour h	MW_e
$E_{\text{over}}(h)$	Surplus electricity (exported or curtailed) at hour h	MW_e
$D_{\text{elec}}(h)$	Baseline (forced) electrical demand at hour h	MW_e
Ancillary Services & Flexibility		
$Q_{\text{req}}(h)$	Grid-requested electrical curtailment in hour h	MW_e
$R_{\text{elec}}(h)$	Delivered electrical curtailment in hour h	MW_e
$R_{\text{heat}}(h)$	Delivered thermal curtailment in hour h	MW_{th}
$R_{\text{shortfall}}(h)$	Shortfall slack for unmet curtailment request in hour h	MW_e
ϕ_{flex}	Flexibility cap: max fraction of $D_{\text{elec}}(h)$ that can be curtailed	–
$P_{\text{reward}}(h)$	Ancillary remuneration rate in hour h	$/MWh
$P_{\text{penalty}}(h)$	Penalty rate for unmet curtailment in hour h	$/MWh
Production & Ramping		
$\psi(h)$	Production throughput (plant output) in hour h	t h^{-1}
ϕ_{prod}	Proportionality factor linking net energy availability to throughput	$(\text{t h}^{-1})/(\text{MW})$
$R_{\text{up}}(h)$	Maximum ramp-up of CHP system	MW_{th}/h
$R_{\text{down}}(h)$	Maximum ramp-down of CHP system	MW_{th}/h
CHP Performance Relationships		
C_{CHP}	Nominal CHP capacity	MW
ρ_{energy}	Fraction of thermal production allocated to electricity conversion	–
$\eta_{\text{electrical}}(h)$	Electrical efficiency of CHP at hour h	–
$\eta_{\text{thermal}}(h)$	Thermal efficiency of CHP at hour h	–
$\alpha_{\text{elec},f}$	Electrical-efficiency base coefficient for fuel f	–
$\beta_{\text{elec},f}$	Electrical-efficiency load coefficient for fuel f	–
$\gamma_{\text{elec},f}$	Electrical-efficiency ambient-temperature coefficient for fuel f	–

$\alpha_{\text{therm},f}$	Thermal-efficiency base coefficient for fuel f	–
$\beta_{\text{therm},f}$	Thermal-efficiency load coefficient for fuel f	–
$\gamma_{\text{therm},f}$	Thermal-efficiency ambient-temperature coefficient for fuel f	–
$T_{\text{ambient}}(h)$	Ambient temperature at hour h	°C
Fuel Use & Blending		
$F_{\text{consumed}}(f,h)$	Fuel f consumed at hour h	MWh
$F_{\text{consumed}}(m)$	Total fuel consumed in month m (monthly aggregate)	MWh
HHV_f	Higher heating value of fuel f	MJ/kg
ΔH_{steam}	Steam enthalpy change per unit mass (if used)	MJ/kg
$B_f(h)$	Fuel blend fraction of fuel f at hour h (or shorthand for $B_f(f,h)$)	–
$B_f(m)$	Fuel blend fraction of fuel f in month m (monthly aggregation)	–
Carbon Capture & Storage (CCS)		
$E_{CO_2}(h)$	Unabated CO_2 emissions at hour h (no capture)	tCO_2/h
$\kappa_{\text{cap}}(h)$	Fraction of CO_2 captured at hour h	–
$E_{\text{captured}}(h)$	CO_2 captured at hour h	tCO_2/h
$E_{\text{uncaptured}}(h)$	Net uncaptured CO_2 emissions at hour h	tCO_2/h
$E_{CO_2,boiler}(h)$	CO_2 emissions from auxiliary boilers at hour h (assumed uncaptured)	tCO_2/h
$Q_{\text{CCS}}(h)$	Reboiler (steam) duty for CCS at hour h	MW_{th}
α_A	Linear coefficient relating captured CO_2 to reboiler duty	MW_{th} / tCO_2
α_B	Nonlinear escalation coefficient in CCS steam requirement	MW_{th}
γ_{ccs}	Diminishing-returns parameter in CCS performance relation	–
$C_{\text{captured}}(m)$	Captured CO_2 in month m	tCO_2
Carbon Trading & Banking		
$C_{\text{free}}(i)$	Free allocation of CO_2 allowances in interval i	tCO_2
$C_{\text{credits}}(i)$	Allowances purchased in interval i	tCO_2
$C_{\text{offset}}(i)$	Offsets used for compliance in interval i	tCO_2
$C_{\text{sold}}(i)$	Allowances sold in interval i	tCO_2
$C_{\text{earned}}(i)$	Surplus allowances earned in interval i	tCO_2
$C_{\text{bank}}(i)$	Banked allowances carried into interval i	tCO_2
$\beta(i)$	Binary: 1 if purchasing allowances in interval i, else 0	–
M	Big-M constant	–
$T_{\max}$	Maximum holding duration for earned allowances	–
$D_{i,j}$	Allowances earned in i disposed (sold/offset) in j	tCO_2
Carbon-Price Solver (Market Clearing)		
$C_{\text{auc}}(y)$	Gross auction volume in year y	tCO_2
$R(y)$	Allowances withdrawn by MSR in year y	tCO_2
$\widetilde{C}_{\text{auc}}(y)$	Net auction supply after MSR in year y	tCO_2
$B(y)$	End-of-year bank of unused allowances in year y	tCO_2
ϕ_{MSR}	MSR withdrawal fraction when bank exceeds threshold	–
Θ	Bank threshold triggering MSR withdrawal	tCO_2
$p(y)$	Market-clearing carbon price in year y	\$/tCO_2
Costs & Objective Terms		
$\mathcal{Z}_1$	Stage 1 total cost	\$
$\mathcal{R}$	Stage 2 net revenue	\$
$P_f(f,m)$	Fuel price for fuel f in month m	\$/MWh
$E_{\text{sold}}(m)$	Electricity exported/sold in month m	MWh
$P_{\text{elec}}^{\text{buy}}(m)$	Electricity purchase price in month m	\$/MWh

$P^{\text{sell}}_{\text{elec}}(m)$	Electricity selling price in month m	\$/MWh
$P^{\text{sell}}_{\text{heat}}(m)$	Heat selling price in month m	\$/MWh$_{\text{th}}$
$P_{\text{credit}}(m)$	Carbon allowance price in month m	\$/tCO_2
$P_{\text{resin}}(h)$	Resin selling price in hour h	\$/t
α_{amine}	Amine solvent OPEX per captured CO_2	\$/tCO_2
α_{liquid}	Solvent makeup OPEX per captured CO_2	\$/tCO_2
$\alpha_{\text{transport}}$	CO_2 transport OPEX per captured CO_2	\$/tCO_2
$\text{CAPEX}_t(m)$	Exogenous unit CAPEX trajectory for technology t in month m	\$/MW
$\text{CAPEX}_t(m,t)$	CAPEX term used in objective for tech t commissioned in month m	\$
Synthetic Scenario Generator Parameters (Appendix)		
τ	Continuous time stamp (market-model clock)	–
τ_0	Base (reference) date/time	–
$\Delta y(\tau)$	Elapsed years since τ_0	yr
$\widehat{Y}_c$	Stabilization year after which commodity growth is capped	yr
$\Delta y^{\star}_c(\tau)$	Capped elapsed years for commodity c	yr
$P_c(\tau_0)$	Nominal price of commodity c at τ_0	\$/MWh
g_c	Annual compound growth rate for commodity c	–
δ_{elec}	Electricity price wedge depth	–
$Y^{\text{elec}}_{\text{stab}}$	Year when electricity wedge reaches plateau	yr
P^{∞}_{elec}	Electricity price plateau	\$/MWh
δ_{h_2}	Hydrogen price wedge depth	–
$Y^{\text{h}_2}_{\text{par}}$	Parity year when hydrogen price locks to electricity plateau	yr
$S_{\text{mon}}(\tau)$	Monthly seasonality factor	–
δ_{winter}	Winter price uplift factor	–
δ_{summer}	Summer price discount factor	–
$\mathcal{M}_{\text{win}}$	Set of winter months	–
$\mathcal{M}_{\text{sum}}$	Set of summer months	–
S^0_{ren}	Initial grid renewable share at τ_0	–
S^1_{ren}	Target grid renewable share by Y^1_{ren}	–
Y^1_{ren}	Year at which S^1_{ren} is reached	yr
$S_{\text{ren}}(\tau)$	Grid renewable share at time τ	–
$Z_c(\tau)$	IID standard-normal draw for commodity c at time τ	–
σ^0_c	Base volatility for commodity c	–
σ_{max}	Maximum electricity volatility cap	–
$\Theta_{\text{ren}}(\tau)$	Normalized renewable progress (0 to 1)	–
$\Theta_{\text{roll}}(\tau)$	Rollout factor for volatility amplification	–
$\sigma_c(\tau)$	Time-varying volatility for commodity c	–
$X_c(\tau)$	Log-normal volatility multiplier for commodity c	–
$\rho^0_{\text{h}_2}$, $\rho^{\text{max}}_{\text{h}_2}$	Base/maximum H_2–electricity correlation	–
$\rho_{\text{h}_2,elec}(\tau)$	Time-varying H_2–electricity correlation	–
ρ^0_{biom}	Base biomass–natural-gas correlation	–
λ_{decay}	Decay rate for biomass–natural-gas correlation	–
$\rho_{\text{biom,ng}}(\tau)$	Time-varying biomass–natural-gas correlation	–
t_{start}, t_{end}	Start/end of a market-event window	–
$\alpha_e(\tau)$	Event multiplier during event window	–
α_e	Scalar event multiplier	–
η_e	Geometric ramp rate for event multiplier	–
$k(\tau)$	Event ramp-step counter	–
ζ^0_{elec}, ζ^1_{elec}	Initial/final electricity emissions intensity	kgCO_2/MWh
$\zeta_{\text{elec}}(\tau)$	Electricity emissions intensity at time τ	kgCO_2/MWh
I_y	Annual inflation rate in year y	–
$I_{\text{cum}}(y)$	Cumulative inflation index through year y	–
$X^{\text{real}}(\tau)$	Real-terms value corresponding to nominal $X(\tau)$	–
$P_{\text{feed},i}(\tau)$	Feedstock price for feedstock i at time τ	\$/t

η_i	Feedstock sensitivity to gas-price deviations	–
$C_{\text{fix}}(\tau)$	Fixed cost component at time τ	\$/t
$P_{\text{resin}}(\tau)$	Resin selling price at time τ	\$/t
$M_{\text{in}}(\tau)$	Resin margin at time τ	\$/t
r	Real discount rate	–
$DF(\tau)$	Discount factor applied to time-τ cash flows	–
$Q_t(y)$	Installed capacity of technology t in year y	MW
g_t	Annual capacity growth rate for technology t	–
r_t^{learn}	Learning-curve rate for technology t	–
γ_t	Learning exponent for technology t	–
$C_t(0)$	Initial CAPEX for technology t (reference)	\$/kW
$Q_t(0)$	Initial capacity for technology t (reference)	MW
$\text{CAPEX}_t^{\text{nom}}(y)$	Nominal CAPEX for technology t in year y	\$/kW
$\text{CAPEX}_t^{\text{real}}(y)$	Real CAPEX for technology t in year y	\$/kW
$\text{CAPEX}_t^{\text{PV}}(y)$	Present-value CAPEX for technology t in year y	\$/kW

CRediT authorship contribution statement

Mahdi Ahmed: Writing – review & editing, Writing – original draft, Visualization, Validation, Software, Resources, Project administration, Methodology, Investigation, Funding acquisition, Formal analysis, Data curation, Conceptualization. **Solomon Brown:** Supervision. **Joan Cordiner:** Writing – review & editing, Supervision.

Declaration of Generative AI and AI-assisted technologies in the writing process

During the preparation of this work, the authors used AI to assist with language editing and improve readability. The authors reviewed and edited the text as needed and take full responsibility for the content of the published article.

Declaration of competing interest

The authors declare that they have no known competing financial interests or personal relationships that could have appeared to influence the work reported in this paper.

Acknowledgment

This work is funded by The University of Sheffield Engineering and Physical Sciences Research Council (EPSRC) Doctoral Training Partnership (DTP).

Appendix A. Scenario generator

Accurately forecasting energy markets decades into the future is notoriously difficult. Instead of attempting to produce a precise forecast, this approach focuses on generating synthetic market trajectories that can flexibly represent a range of potential and correlated events. This strategy acknowledges the inherent uncertainty in projecting exact prices and technology developments over long horizons. Energy systems are subject to policy-driven shifts and volatile interactions among commodities, making scenario-based analysis critical for evaluating investment strategies.

A key feature of this framework is the preservation of realistic linkages among commodities by embedding correlations and volatility behaviors. For instance, shocks in natural gas prices can propagate through related commodities such as biomass and electricity, mirroring real-world interactions. This is essential for stress-testing decarbonization strategies under diverse policy and market conditions. Moreover, the ability to modify parameters such as renewable energy penetration, carbon tax rates, or exchange rate volatility provides a powerful tool for “what-if” analyses, facilitating decision-making under uncertainty.

Investment evaluation and financial metrics

All investments are evaluated on a net present value (NPV) basis. All future cash flows, including retrofit CAPEX, modified OPEX, carbon compliance costs, and ancillary revenues, are first expressed in real (inflation-adjusted) terms and then discounted using an annual real discount rate r. Specifically, a cash flow occurring t years in the future is adjusted by the factor

$$DF(t) = \frac{1}{(1+r)^t}.$$

This approach provides a rigorous basis for our DCF analysis and allows us to compute the internal rate of return (IRR)–the discount rate that zeros the NPV. In practice, investments in large-scale chemical retrofits are benchmarked against a risk-adjusted hurdle rate, often set around 15%, which represents a premium over the firm’s WACC. An IRR exceeding this threshold indicates that the project generates returns that justify the inherent risks and the substantial upfront capital commitment.

A.1. Base prices and compound growth

Let τ_0 be the base date:

$$\Delta y(\tau) = \mathrm{year}(\tau) - \mathrm{year}(\tau_0), \quad \Delta y_c^\star(\tau) = \min\left[\Delta y(\tau),\, \hat{Y}_c - \mathrm{year}(\tau_0)\right].$$

For each commodity $c \in \{\mathrm{elec}, \mathrm{ng}, \mathrm{h_2}, \mathrm{biom}\}$, let $P_c(\tau_0)$ denote its nominal price at τ_0. Natural gas and biomass follow compound growth:

$$P_c^{\mathrm{grow}}(\tau) = P_c(\tau_0)\left(1 + g_c\right)^{\Delta y_c^\star(\tau)}, \quad c \in \{\mathrm{ng}, \mathrm{biom}\}, \tag{46}$$

where g_c is the annual growth rate and $\Delta y_c^\star$ caps growth after stabilization year $\hat{Y}_c$.

Electricity uses a linear decarbonisation wedge down to a plateau:

$$P_{\mathrm{elec}}^{\mathrm{grow}}(\tau) = P_{\mathrm{elec}}(\tau_0)\left[1 - \delta_{\mathrm{elec}}\,\frac{\Delta y(\tau)}{Y_{\mathrm{stab}}^{\mathrm{elec}} - \mathrm{year}(\tau_0)}\right]_+, \quad [x]_+ = \max(x, 0), \tag{47}$$

with plateau

$$P_{\mathrm{elec}}^{\infty} = P_{\mathrm{elec}}(\tau_0)\,(1 - \delta_{\mathrm{elec}}).$$

Green hydrogen mirrors the wedge until parity year $Y_{\mathrm{par}}^{\mathrm{h_2}}$, then locks to the electricity plateau:

$$P_{\mathrm{h_2}}^{\mathrm{grow}}(\tau) = \begin{cases} P_{\mathrm{h_2}}(\tau_0)\left[1 - \delta_{\mathrm{h_2}}\,\frac{\Delta y(\tau)}{Y_{\mathrm{par}}^{\mathrm{h_2}} - \mathrm{year}(\tau_0)}\right], & \mathrm{year}(\tau) \le Y_{\mathrm{par}}^{\mathrm{h_2}}, \\ P_{\mathrm{elec}}^{\infty}, & \text{otherwise}. \end{cases} \tag{48}$$

A.2. Seasonality

Define the monthly factor

$$S_{\mathrm{mon}}(\tau) = \begin{cases} 1 + \delta_{\mathrm{winter}}, & \mathrm{month}(\tau) \in \mathcal{M}_{\mathrm{win}}, \\ 1 - \delta_{\mathrm{summer}}, & \mathrm{month}(\tau) \in \mathcal{M}_{\mathrm{sum}}, \\ 1, & \text{otherwise}, \end{cases}$$

where $\mathcal{M}_{\mathrm{win}}$ and $\mathcal{M}_{\mathrm{sum}}$ are winter and summer months. Then

$$P_c^{\mathrm{sea}}(\tau) = S_{\mathrm{mon}}(\tau)\,P_c^{\mathrm{grow}}(\tau), \quad c \in \{\mathrm{elec}, \mathrm{ng}\}.$$

A.3. Renewable-share trajectory

Let S_{ren}^0 be the grid's renewable fraction at τ_0, rising linearly to S_{ren}^1 by year Y_{ren}^1:

$$S_{\mathrm{ren}}(\tau) = S_{\mathrm{ren}}^0 + \left(S_{\mathrm{ren}}^1 - S_{\mathrm{ren}}^0\right)\frac{\Delta y(\tau)}{Y_{\mathrm{ren}}^1 - \mathrm{year}(\tau_0)}. \tag{49}$$

A.4. Volatility modeling

For each commodity draw $Z_c(\tau) \sim \mathcal{N}(0, 1)$ and define

$$X_c(\tau) = \exp\left[\sigma_c(\tau)\,Z_c(\tau)\right], \tag{50}$$

so that

$$P_c^{\mathrm{vol}}(\tau) = P_c^{\mathrm{sea}}(\tau)\,X_c(\tau). \tag{51}$$

Hourly volatility for electricity increases with renewables:

$$\sigma_{\mathrm{elec}}(\tau) = \sigma_{\mathrm{elec}}^0 + \left(\sigma_{\max} - \sigma_{\mathrm{elec}}^0\right)\Theta_{\mathrm{ren}}(\tau)\,\Theta_{\mathrm{roll}}(\tau), \tag{52}$$

where

$$\Theta_{\mathrm{ren}}(\tau) = \frac{S_{\mathrm{ren}}(\tau) - S_{\mathrm{ren}}^0}{S_{\mathrm{ren}}^1 - S_{\mathrm{ren}}^0}, \tag{53}$$

and $\Theta_{\mathrm{roll}}(\tau)$ linearly phases this effect in. For $c \in \{\mathrm{ng}, \mathrm{h_2}, \mathrm{biom}\}$, $\sigma_c(\tau) = \sigma_c^0$.

A.5. Time-varying correlations

The cross-commodity correlations evolve as

$$\rho_{\mathrm{h_2,elec}}(\tau) = \rho_{\mathrm{h_2}}^0 + \left(\rho_{\mathrm{h_2}}^{\max} - \rho_{\mathrm{h_2}}^0\right)\Theta_{\mathrm{ren}}(\tau), \tag{54}$$

$$\rho_{\mathrm{biom,ng}}(\tau) = \rho_{\mathrm{biom}}^0\left[1 - \lambda_{\mathrm{decay}}\,\Theta_{\mathrm{ren}}(\tau)\right]. \tag{55}$$

These feed into blended prices:

$$P_{\mathrm{h_2}}^{\mathrm{cor}}(\tau) = \left[1 - \rho_{\mathrm{h_2,elec}}(\tau)\right]P_{\mathrm{h_2}}^{\mathrm{vol}}(\tau) + \rho_{\mathrm{h_2,elec}}(\tau)\,P_{\mathrm{elec}}^{\mathrm{vol}}(\tau), \tag{56}$$

$$P_{\mathrm{biom}}^{\mathrm{cor}}(\tau) = \left[1 - \rho_{\mathrm{biom,ng}}(\tau)\right]P_{\mathrm{biom}}^{\mathrm{vol}}(\tau) + \rho_{\mathrm{biom,ng}}(\tau)\,P_{\mathrm{ng}}^{\mathrm{vol}}(\tau). \tag{57}$$

A.6. Market events and policy multipliers

For any commodity c during an event window $\tau_{\text{start}} \le \tau \le \tau_{\text{end}}$, apply

$$P_c(\tau) \leftarrow \alpha_e(\tau)\, P_c(\tau), \quad \alpha_e(\tau) = \begin{cases} \alpha_e, & \text{scalar event,} \\ (1+\eta_e)^{k(\tau)},\ k(\tau) = \text{no. of ramp steps,} & \text{geometric ramp.} \end{cases}$$

A.7. Emissions intensities

Electricity emissions intensity declines with renewables:

$$\zeta_{\text{elec}}(\tau) = \zeta^0_{\text{elec}} - \left(\zeta^0_{\text{elec}} - \zeta^1_{\text{elec}}\right) \Theta_{\text{ren}}(\tau),$$

optionally scaled up during peak-demand hours. Natural gas and hydrogen follow nonlinear transitions between defined endpoints; biomass intensity ζ_{biom} remains constant.

A.8. Inflation adjustment

Given annual inflation rates I_y, define the cumulative index

$$I_{\text{cum}}(y) = \prod_{\kappa=\text{year}(\tau_0)}^{y} (1 + I_\kappa).$$

Every monetary variable (prices, taxes, CAPEX) is converted to real terms by

$$X^{\text{real}}(\tau) = \frac{X(\tau)}{I_{\text{cum}}\left(\text{year}(\tau)\right)}.$$

A.9. Feedstock, resin and margin

Feedstock prices P_{BPA} and P_{ECH} track natural-gas deviations:

$$P_{\text{feed},i}(\tau) = P_{\text{feed},i}(\tau_0) + \eta_i \left[P_{\text{ng}}(\tau) - P_{\text{ng}}(\tau_0)\right], i \in \{\text{BPA}, \text{ECH}\}.$$

Resin selling price $P_{\text{resin}}(\tau)$ follows a GBM with optional event multipliers.

$$M_{\text{in}}(\tau) = P_{\text{resin}}(\tau) - \left[P_{\text{feed}}(\tau) + C_{\text{fix}}(\tau)\right], \tag{58}$$

and its present-value uses real discount factor

$$DF(\tau) = (1+r)^{-\Delta y(\tau)}.$$

A.10. CAPEX learning curves

For technology k, annual capacity evolves

$$Q_k(y+1) = Q_k(y)\left(1 + g_k\right),$$

with learning exponent

$$\gamma_k = \frac{\ln\left(1 - r_k^{\text{learn}}\right)}{\ln 2}.$$

Nominal CAPEX is

$$\text{CAPEX}_k^{\text{nom}}(y) = C_k(0)\left[\frac{Q_k(y)}{Q_k(0)}\right]^{\gamma_k}, \tag{59}$$

converted to real and present-value terms by

$$\text{CAPEX}_k^{\text{real}}(y) = \frac{\text{CAPEX}_k^{\text{nom}}(y)}{I_{\text{cum}}(y)}, \quad \text{CAPEX}_k^{\text{PV}}(y) = \text{CAPEX}_k^{\text{real}}(y)\,(1+r)^{-(y-\text{year}(\tau_0))}.$$

Base parameters used for determining CAPEX are shown in Appendix Table 12.

Appendix B. Grid-flex event generation

B.1. Overview

The actual curtailed energy $R_{\text{elec}}(h)$ and any shortfall $R_{\text{shortfall}}(h)$ enters the optimization via Eqs. (7)–(8), with:

$$Q_{\text{req}}(h) = E(h)\,\hat{R}(h)\,. \tag{60}$$

$$R_{\text{elec}}(h) \le \phi_{\text{flex}}\, D_{\text{elec}}(h), \tag{61}$$

Table 8
Stochastic variables and default values, All numerical values are calibrated to the following publicly available sources [57–60].

Symbol	Description	Default/Distribution
ϕ_{flex}	Flexibility index (max fraction of demand curtailable)	scenario-specific
p_0, $p_{\max}$, $p_{\min}$	Base, peak, floor call probabilities	0.004, 0.012, 0.002
k_1, k_2	Steepness of the probability curve	10
α_ϕ	Flexibility-scaling factor for call probability	0.5
σ_R	Log-normal spread of curtailment request size	0.35
c_{SIP}	Strike-price multiplier on SIP	$U(0.6, 1.2)$
λ	Penalty multiplier on LMP	1.5
ϵ_{reward}, $\epsilon_{\text{penalty}}$	Pricing noise	$\mathcal{N}(0, 0.05^2)$
SIP(h), LMP(h)	Market price inputs	Exogenous series

B.2. Call probability

The baseline probability of a flex-call is

$$p_{\text{ev}}(h) = p_0 + (p_{\max} - p_0)\frac{1}{1+\exp\left[-k_1\,(\Theta_{\text{ren}}(h) - 0.5)\right]} - (p_{\max} - p_{\min})\frac{1}{1+\exp\left[-k_2\,(\Theta_{\text{ren}}(h) - 0.5)\right]}, \tag{62}$$

To reflect that more-flexible plants are called more often, this probability is scaled by the plant's flexibility index ϕ_{flex} (maximum fraction of $D_{\text{elec}}(h)$ curtailable):

$$\tilde{p}_{\text{ev}}(h) = \min\left\{1,\ p_{\text{ev}}(h)\,[1 + \alpha_\phi\,\phi_{\text{flex}}]\right\}, \quad \alpha_\phi = 0.5. \tag{63}$$

A single draw $u \sim U(0,1)$ then determines

$$E(h) = \begin{cases} 1, & u < \tilde{p}_{\text{ev}}(h), \\ 0, & \text{otherwise.} \end{cases}$$

B.3. Proposed curtailment

When $E(h) = 1$, the requested curtailment $\widehat{R}(h)$ (MWh) is sampled from a log-normal distribution truncated at the plant's technical limit:

$$\widehat{R}(h) \sim \text{LogNormal}(\mu_R, \sigma_R^2), \quad 0 < \widehat{R}(h) < \phi_{\text{flex}}\,D_{\text{elec}}(h), \tag{64}$$

where $D_{\text{elec}}(h)$ is the baseline demand and

$$\sigma_R = 0.35, \qquad \mu_R = \ln\big(0.30\,D_{\text{elec}}(h)\big) - \tfrac{1}{2}\sigma_R^2.$$

If $E(h) = 0$, then $\widehat{R}(h) = 0$.

B.4. Pricing

The remuneration and penalty rates are given by

$$P_{\text{reward}}(h) = c_{SIP}\,\text{SIP}(h) + \epsilon_{\text{reward}}(h), \qquad \epsilon_{\text{reward}}(h) \sim \mathcal{N}(0, 0.05^2), \tag{65}$$

$$P_{\text{penalty}}(h) = \max\left[P_{\text{reward}}(h),\ \lambda\,\text{LMP}(h)\right] + \epsilon_{\text{penalty}}(h), \qquad \epsilon_{\text{penalty}}(h) \sim \mathcal{N}(0, 0.05^2). \tag{66}$$

Parameters involved for all ancillary market call generations are in Appendix Table 8.

Appendix C. Methodology for decoupling production from seasonal thermal demand

Given the influence of ambient temperature on thermal demand, Heating Degree Days (HDD) are used to model and adjust for these seasonal effects, as otherwise seasonal-led variations in thermal demand would correspond to differing production rates.

Historical temperature data are sourced from the UK Met Office, providing hourly records across multiple years to capture seasonal trends [61].

C.1. Heating degree days calculation

Heating Degree Days (HDD) quantify the heating requirement based on ambient temperature, calculated as:

$$\text{HDD}(h) = \max(0, T_{\text{base}} - T(h)), \tag{67}$$

where $T_{\text{base}} = 15.5\,°\text{C}$ is the base temperature (standard for UK building heating thresholds), and $T(h)$ is the hourly ambient temperature. Daily HDD values are typically summed from hourly calculations for analysis.

Table 9
Exogenous EU ETS inputs for key years ($MtCO_2$). Italicized entries are interpolated to 2050.

Variable	2025	2030	*2035*	*2050*
Statutory cap C_{cap}	1298	825	*620*	*0*
Auction volume C_{auc}	740	471	*354*	*0*
Free allocation C_{free}	558	354	*266*	*0*
Initial bank $B(2024)$	1112	–	–	–
MSR intake rate ϕ_{MSR}	24%	24%	*12%*	–
MSR threshold Θ	833	833	833	–

C.2. Correlation

Thermal demand is modeled as a linear function of HDD:

$$D_{\text{heat}}(h) = a + b \cdot \text{HDD}(h), \tag{68}$$

where a (intercept) and b (slope) are parameters estimated with linear regression. Historical thermal demand data are fit with corresponding HDD values.

C.3. Decoupling

To remove seasonal effects, a normalization factor γ_s is introduced:

$$\gamma_s = \frac{\frac{1}{|\mathcal{H}_s|}\sum_{h\in\mathcal{H}_s}\text{HDD}(h)}{\frac{1}{|\mathcal{H}|}\sum_{h\in\mathcal{H}}\text{HDD}(h)}, \tag{69}$$

where $\mathcal{H}_s$ represents hours in season s (e.g., winter months), and $\mathcal{H}$ includes all hours in the year. This factor scales seasonal HDD averages relative to the annual average, dampening seasonal peaks. The normalized thermal demand is then:

$$D^{\text{norm}}_{\text{heat}}(h) = a + b \cdot \left(\frac{\text{HDD}(h)}{\gamma_s}\right), \quad \forall h \in \mathcal{H}_s, \tag{70}$$

yielding a demand profile independent of seasonal temperature variations.

C.4. Implementation and validation

The normalized demand $D^{\text{norm}}_{\text{heat}}(h)$ is integrated into production planning models to adjust throughput. Validation involves comparing production stability pre- and post-normalization using metrics such as demand variance or regression R^2, confirming the methodology's effectiveness with historical data.

Appendix D. Carbon-market inputs

All numerical values (Table 9) are taken from official EU legislation or Commission reports, with extrapolations to 2050 where necessary [62–64].

D.1. Exogenous EU ETS parameters

The statutory cap $C_{\text{cap}}(y)$ in our model follows the linear reduction factor (LRF) mandated under Phase IV of the EU ETS. From 2025 onward we apply a constant annual LRF of 4.3:

$$C_{\text{cap}}(y) = C_{\text{cap}}(y-1)\,(1-0.043), \quad y \geq 2025, \tag{71}$$

with $C_{\text{cap}}(2024) = 1,298\ MtCO_2$ taken from the Phase IV schedule [63]. Beyond 2030, no official cap values are published, and so the cap is linearly phased to zero by 2050 to reflect the EU's net-zero target:

$$C_{\text{cap}}(y) = C_{\text{cap}}(2030)\,\frac{2050-y}{20}, \quad 2030 \leq y \leq 2050. \tag{72}$$

Under the same Phase IV rules, 57% of allowances are auctioned each year and 43% are freely allocated to industry:

$$C_{\text{auc}}(y) = 0.57\,C_{\text{cap}}(y), \quad C_{\text{free}}(y) = 0.43\,C_{\text{cap}}(y). \tag{73}$$

Free allocation is phased to zero by 2035 by linearly reducing the 43% share to 0 over 2031–2035, capturing the impact of CBAM.
The TNAC (total number of allowances in circulation) at end of 2023 was 1112 $MtCO_2$, which we adopt as the initial bank:

$$B(2024) = 1112\ \text{Mt}. \tag{74}$$

The MSR modifies annual supply based on the bank $B(y)$. Per Decision 2015/1814, we use an intake rate $\phi_{\text{MSR}} = 0.24$ and threshold $\Theta = 833$ $MtCO_2$ [62]:

$$\phi_{\text{MSR}} = 0.24, \quad \Theta = 833\ MtCO_2. \tag{75}$$

D.2. Banking and MSR feedback mechanism

At the start of each year y, the net volume of allowances available to the market is

$$\widetilde{C}_{\mathrm{auc}}(y) = C_{\mathrm{auc}}(y) - R(y), \tag{76}$$

where $R(y)$ is the MSR withdrawal defined by

$$R(y) = \phi_{\mathrm{MSR}}\ \max\left[B(y-1) - \Theta, 0\right]. \tag{77}$$

Firms surrender allowances equal to their emissions $E(y,p)$ at the clearing price p. The bank is updated as

$$B(y) = B(y-1) + \widetilde{C}_{\mathrm{auc}}(y) - E(y, p(y)). \tag{78}$$

D.3. Clearing-price determination via bisection

To find the market-clearing price $p(y)$, we use a bisection search over $[p_{\mathrm{low}}, p_{\mathrm{high}}]$. At each candidate price the cohort's emissions $E(y,p)$ are computed by solving each plant's decarbonization optimization. We iterate until

$$\left|E(y,p) - \widetilde{C}_{\mathrm{auc}}(y)\right| \le \varepsilon_C\ \widetilde{C}_{\mathrm{auc}}(y), \tag{79}$$

with plateau detection tolerances ε_E guiding bracket adjustments (see Algorithm 1).

D.4. Clearing-price algorithm

Clearing-Price Search Algorithm

Algorithm 1 Yearly price–emissions clearing.

for $t = 1$ **to** T **do**
  Compute $\widetilde{C} \leftarrow \widetilde{C}_{\mathrm{auc}}(t)$
  Initialize price bounds $[p_{\mathrm{low}}, p_{\mathrm{high}}]$
  repeat
    $p \leftarrow \frac{p_{\mathrm{low}}+p_{\mathrm{high}}}{2}$
    Solve each plant's decision at p and at $p \pm \delta p$
    $E \leftarrow S\, e(t,p)$
    $E^{+} \leftarrow S\, e(t, p+\delta p)$
    $E^{-} \leftarrow S\, e(t, p-\delta p)$
    if $|E^{+} - E| \le \varepsilon_E$ **then** ▷ flat plateau above
      $p_{\mathrm{low}} \leftarrow p$
    else if $|E^{-} - E| \le \varepsilon_E$ **then** ▷ flat plateau below
      $p_{\mathrm{high}} \leftarrow p$
    else
      if $E > \widetilde{C}$ **then**
        $p_{\mathrm{low}} \leftarrow p$
      else
        $p_{\mathrm{high}} \leftarrow p$
      end if
    end if
  until $|E - \widetilde{C}| \le \varepsilon_C\, \widetilde{C}$
  Set $p(t) \leftarrow p$ and $E(t) \leftarrow E$
  Update $B(t)$ via Eq. (42) and $R(t+1)$ via Eq. (43)
end for

This algorithm yields, for any scenario of constrained or delayed decarbonization, the carbon-price path $p(t)$ required to induce abatement, to quantify both the policy stringency needed and the resulting feedback on the allowance market.

Appendix E. Additional tables

Table 10
Simulation scenarios and model modifications.

Scenario	Modifications
Base-case	• Central forecasts for commodity prices, demand, volatility, and policy variables (see Table 3).
Scenario A: Infrastructure Limitations	• Electric-boiler investment disabled: $x^{(EB)}_{invest,m} = 0$.
Scenario B: Delayed Grid Decarbonisation	• Renewable share still targets $S^1_{ren} = 0.80$ but is reached in $Y^1_{ren} = 2050$. • Electricity-price wedge stabilises in $Y^{elec}_{stab} = 2050$. • Volatility roll-back window $y_{red,0} = 2050$–$y_{red,1} = 2060$ with $\sigma_0 = 0.05$, $\sigma_{max} = 0.25$. • Slower correlation shift: $\rho^0_{h_2} = 0.10$, $\rho^{max}_{h_2} = 0.80 \Rightarrow \rho_{elec,h2}(t) \le 0.30$ until 2045; $\rho^0_{biom} = 0.45$, $\lambda_{decay} = 0.5 \Rightarrow \rho_{elec,ng}(t) \ge 0.60$ until 2045. • Grid CO_2 intensity declines linearly from $\zeta^0_{elec} = 0.35$ to $\zeta^1_{elec} = 0.05\ \mathrm{kg\,CO_2/kWh}$ over 2025–2050.
Scenario C: No Banking	• Carbon-credit holding horizon suppressed: $T_{max} = 0$.
Scenario D: Forced CCS Uptake	• Incrementally raise the effective carbon price $P^{eff}_{CO_2}$ until the optimiser selects CCS.

Table 11
Additional parameters required for replication.

Category	Symbol	Value(s)	Unit	Notes/Source
Lognormal volatilities				
Electricity base/max σ	σ_0, σ_{max}	0.05, 0.25	–	Renewable-linked σ (Eq. B.6).
Natural gas σ	σ^0_{ng}	0.07	–	Constant σ.
Biomass σ	σ^0_{biom}	0.10	–	Constant σ.
Hydrogen σ	$\sigma^0_{h_2}$	0.10	–	Constant σ.
Volatility roll-back window				
Start/end year	$y_{red,0}$, $y_{red,1}$	2035/2045	–	Shifts to 2050/2060 in Scenario B.
Seasonality multipliers				
Winter uplift	δ_{winter}	+0.10	–	Months 12-02.
Summer discount	δ_{summer}	−0.05	–	Months 06-08.
FX process (USD vs. plant currency)				
Drift μ_{FX}	–	0.02	yr^{-1}	Long-run USD weakening [45].
Volatility σ_{FX}	–	0.10	–	Hourly σ in GBM.

Table 12
Installed CAPEX for Decarbonization Technologies in EU/UK (2025 vs. 2055).

Technology	**2025 CAPEX**	**2055 CAPEX**	Notes/Source
Electric boiler	\$230/kW	\$200/kW	Base installed-cost context and commercial sizing drawn from DOE/MESC tip sheet [65]. Nominal investment set to 0.15 M\$/MW_{th}, with +30% steam-service penalty (site integration) and 0.085 M\$/MW grid-connection (site-specific allowance). 2055 value applies an assumed learning reduction.
Hydrogen CHP retrofit	\$550/kW	\$450/kW	Retrofit CAPEX set as refurbishment cost (300\$/kW) plus balance-of-plant modifications; anchored against typical CHP installed-cost magnitudes in EPA catalog (order-of-magnitude consistency) [66]. 2055 value applies an assumed cost reduction.
CCS system (fossil-fuel power)	\$168/tCO_2·yr	\$141/tCO_2·yr	Capture cost representation aligned with published capture cost studies and techno-economic baselines [67,68]. 2055 value applies an assumed learning reduction.

Table 13
CCS parameters and unit costs for a UK plant with offshore storage (liquefaction included in transport).

Category	Symbol	Value(s)	Unit	Notes/Source
CCS process parameters				
Linear reboiler duty coefficient	α_A	970	kWh/tCO_2	Matches typical 30 wt% MEA specific reboiler duty around 3.4–3.6 GJ/tCO_2 at ∼90% capture [69].
Nonlinear escalation coefficient	α_B	200	kWh	Parameterised to reproduce duty increase as capture fraction approaches 1; consistent with higher-duty behaviour at very high capture rates [69].
Diminishing-return parameter	γ_{ccs}	0.50	–	Shape parameter for rising marginal duty near full capture [69].
CO_2 abatement cost components				
Amine-makeup chemical cost	α_{amine}	5.0	\$/tCO_2	Based on an assumed MEA loss rate and unit chemical price; included as minor OPEX component (assumption, sensitivity-tested).
Transport (incl. liquefaction)	$\alpha_{transport}$	20	\$/tCO_2	Order-of-magnitude consistent with transport/liquefaction cost components in technology catalogues for CO_2 transport chains [68].
Storage injection cost	$\alpha_{storage}$	6	\$/tCO_2	Within published storage-cost ranges for onshore/offshore scenarios (site-dependent) [70].

Data availability

Data will be made available on request.

References

[1] International Energy Agency. Industry. 2023, https://www.iea.org/energy-system/industry, [Accessed May 2025].
[2] Bouckaert S, Pales AF, McGlade C, Remme U, Wanner B, Varro L, D'Ambrosio D, Spencer T. Net zero by 2050: A roadmap for the global energy sector. 2021.
[3] McKinsey & Company. Decarbonization of industrial sectors: The next frontier. 2017, https://www.mckinsey.com/industries/oil-and-gas/our-insights/decarbonization-of-industrial-sectors-the-next-frontier, [Accessed May 2025].
[4] Borghesi S, Pahle M, Perino G, Quemin S, Willner M. The market stability reserve in the EU emissions trading system: A critical review. Annu Rev Resour Econ 2023;15:131–52. http://dx.doi.org/10.1146/annurev-resource-111820-030145.
[5] UK Government and European Commission. UK–EU summit: Common understanding. 2025, https://www.gov.uk/government/publications/ukeu-summit-key-documentation/uk-eu-summit-common-understanding-html, (Published 19 May 2025).
[6] European Parliamentary Research Service. Linking the EU and UK emissions trading systems. Tech. rep., EPRS; 2025, URL https://www.europarl.europa.eu/RegData/etudes/BRIE/2025/775873/EPRS_BRI(2025)775873_EN.pdf.
[7] ICAP. EU and UK commit to linking emissions trading systems. 2025, https://icapcarbonaction.com/en/news/eu-and-uk-commit-linking-emissions-trading-systems-landmark-cooperation-agreement, News release, 22 May 2025.
[8] European Parliament and Council of the European Union. Regulation (EU) 2023/956 of the European Parliament and of the Council of 10 May 2023 establishing a carbon border adjustment mechanism. Off J Eur Union 2023;L 130:52–104, URL https://eur-lex.europa.eu/eli/reg/2023/956/oj/eng, OJ L 130, 16.5.2023, 52–104.
[9] European Commission. Carbon border adjustment mechanism (CBAM) portal. 2025, https://taxation-customs.ec.europa.eu/carbon-border-adjustment-mechanism_en.
[10] Trevisan S, Buchbjerg B, Guedez R. Power-to-heat for the industrial sector: Techno-economic assessment of a molten salt-based solution. Energy Convers Manage 2022;269:116103, URL https://www.sciencedirect.com/science/article/pii/S0196890422011402.
[11] Kockel C, Kulawik J, Wohlleben D. Which way to choose? A generic modular life cycle assessment for hydrogen production and import pathways to Germany. Energy J 2024;45(SI1). http://dx.doi.org/10.5547/01956574.45.SI1.ckoc, URL https://journals.sagepub.com/doi/abs/10.5547/01956574.45.SI1.ckoc.
[12] Sharifzadeh M, Cooper N, van't Noordende H. Operational strategies and integrated design for producing green hydrogen from wind electricity. Int J Hydrog Energy 2024. URL https://www.sciencedirect.com/science/article/pii/S0360319924010784.
[13] Duong C, Bower C, Hume K, Rock L, Tessarolo S. Quest carbon capture and storage offset project: Findings and learnings from 1st reporting period. Int J Greenh Gas Control 2019;89:65–75.
[14] Nwachukwu CM, Toffolo A, Wetterlund E. Biomass-based gas use in Swedish iron and steel industry–supply chain and process integration considerations. Renew Energy 2020;156:1258–71, URL https://www.sciencedirect.com/science/article/pii/S096014811931287X.
[15] Miehling S, Hanel A, Lambert J, Fendt S, Spliethoff H. Energy system optimisation using (mixed integer) linear programming. 2023, arXiv preprint arXiv:2308.01882, URL https://arxiv.org/abs/2308.01882.
[16] Huynh LT, Ierapetritou M. Robust design of biorefineries under environmental policy and market uncertainty. Appl Energy 2024;376:124283. http://dx.doi.org/10.1016/j.apenergy.2024.124283.
[17] Yáñez J, Martínez JD, Rivero R, et al. CO_2 mitigation strategy for a refinery: Techno-economic assessment of process modifications and carbon capture. Energy 2022;254:124349. http://dx.doi.org/10.1016/j.energy.2022.124349.
[18] Verdolini E, Torreggiani L, Giarola S, Tavoni M, Hafstead M. Industrial deep decarbonization: Modeling approaches and data challenges. 2023, Resources for the Future Report 23-10, URL https://www.rff.org/publications/reports/industrial-deep-decarbonization-modeling-approaches-and-data-challenges/.
[19] Shen Y, Zhang B, Li X, Wang J, Shahidehpour M. Data-driven adaptive robust optimization for industrial energy systems planning with renewable integration. Appl Energy 2022;307:118148. http://dx.doi.org/10.1016/j.apenergy.2021.014239.
[20] Wang P, Papadokonstantakis S. Multi-period stochastic optimization of integrating CCS/CCU for the cement industry. In: Computer aided chemical engineering. Elsevier; 2024, http://dx.doi.org/10.1016/B978-0-443-28824-1.50351-3, Chapter.
[21] Giannikopoulos IA, Sadri M, Koeh P, Engell S. Thermal electrification of chemical processes: Process modifications with renewable electricity and storage. Ind Eng Chem Res 2024. http://dx.doi.org/10.1021/acs.iecr.4c00737.
[22] Zhang Q, Wang Y, Li Q, Gao X. Optimal retrofitting of conventional oil refinery to co-process biomass feedstock under uncertainty. AIChE J 2024;70(e18371). http://dx.doi.org/10.1002/aic.18371.
[23] Chew YE, How BS, Sunarso J, Moser I. Decarbonization of energy operations for hard-to-abate industries through smart energy system optimization. Clean Technol Environ Policy 2025. URL https://link.springer.com/article/10.1007/s41660-025-00494-y.
[24] Guo J, Zhou Y. Low-carbon planning of a cement integrated energy system considering carbon allowance and green certificates trading. Processes 2023;11(4):1219. http://dx.doi.org/10.3390/pr11041219.
[25] Neuwirth M, Fleiter T, Hofmann R. Modelling the transformation of energy-intensive industries based on site-specific investment decisions. Sci Rep 2024;14(30552). http://dx.doi.org/10.1038/s41598-024-78881-7.
[26] Fleiter T, Rehfeldt M, Herbst A, Elsland R, Klingler A-L, Manz P, Eidelloth S. A methodology for bottom-up modelling of energy transitions in the industry sector: The FORECAST model. Energy Strat Rev 2018;22:237–54. http://dx.doi.org/10.1016/j.esr.2018.09.005.
[27] Richstein JC, Chappin EJL, de Vries LJ. The market (in-)stability reserve for EU carbon emission trading: Why it might fail and how to improve it. Energy Policy 2015;76:125–35. http://dx.doi.org/10.1016/j.enpol.2014.10.033.
[28] Richstein JC, Chappin EJL, de Vries LJ. Cross-border electricity market effects due to price caps in an emission trading system: An agent-based approach. Energy Policy 2014;71:139–58. http://dx.doi.org/10.1016/j.enpol.2014.04.009.
[29] Ouassou JA, Reigstad G, Wolfgang O. Applying endogenous learning models in energy system optimization. Energies 2021;14(16):4819. http://dx.doi.org/10.3390/en14164819.
[30] Zeyen E, Victoria M, Brown T. Endogenous learning for green hydrogen in a sector-coupled energy model for europe. Nat Commun 2023;14(3743). http://dx.doi.org/10.1038/s41467-023-39397-2.
[31] Xu Z. The electricity market design for decentralized flexibility sources. Oxf Work Pap Ser 2019.
[32] Gulotta F, Daccò E, Bosisio A. Opening of ancillary service markets to distributed energy resources: A review. Energies 2023;16(6):2814.
[33] de Santoli L, Basso GL, Bruschi D. Energy characterization of CHP (combined heat and power) fuelled with hydrogen enriched natural gas blends. Energy 2013;57:231–40, URL https://www.sciencedirect.com/science/article/pii/S0360544213005999.
[34] Keirstead J, Samsatli N, Shah N, Weber C. The impact of CHP (combined heat and power) planning restrictions on the efficiency of urban energy systems. Energy 2012;41:93–103, URL https://www.sciencedirect.com/science/article/pii/S0360544211003884.
[35] Zhao T, Liu Z. Investment timing analysis of hydrogen-refueling stations and the case of China: Independent or co-operative investment? Energies 2023;16(13):5032, URL https://www.mdpi.com/1996-1073/16/13/5032.
[36] Liu J, Zhang Q, Teng F, Wang L, Gao Z. A new investment decision-making model of hydrogen energy storage technology based on real-time operation optimization and learning effects. Energy Rep 2024. URL https://www.sciencedirect.com/science/article/pii/S2352152X24023314.
[37] Isogai H, Nakagaki T. Power-to-heat amine-based post-combustion CO2 capture system with solvent storage utilizing fluctuating electricity prices. Appl Energy 2024;368:123519. http://dx.doi.org/10.1016/j.apenergy.2024.123519, URL https://www.sciencedirect.com/science/article/pii/S0306261924009024.
[38] Bertone M, Stabile L, Cortellessa G, Arpino F, Buonanno G. Techno-economic assessment of amine-based carbon capture in waste-to-energy incineration plant retrofit. Sustainability 2024;16(19). http://dx.doi.org/10.3390/su16198468, URL https://www.mdpi.com/2071-1050/16/19/8468.
[39] Mostafavi E, Ashrafi O, Navarri P. Assessment of process modifications for amine-based post-combustion carbon capture processes. Clean Eng Technol 2021;4:100249. http://dx.doi.org/10.1016/j.clet.2021.100249, URL https://www.sciencedirect.com/science/article/pii/S2666790821002093.
[40] Nessi E, Papadopoulos AI, Seferlis P. A review of research facilities, pilot and commercial plants for solvent-based post-combustion CO2 capture: Packed bed, phase-change and rotating processes. Int J Greenh Gas Control 2021;111:103474. http://dx.doi.org/10.1016/j.ijggc.2021.103474, URL https://www.sciencedirect.com/science/article/pii/S1750583621002267.
[41] ICAP. Emissions trading worldwide. 2024, URL https://icapcarbonaction.com/system/files/document/240522_report_final.pdf.

[42] Hart WE, Watson J-P, Woodruff DL. Pyomo: modeling and solving mathematical programs in Python. Math Program Comput 2011;3(3):219–60. http://dx.doi.org/10.1007/s12532-011-0026-8.
[43] Gurobi Optimization, LLC. Gurobi optimizer reference manual. 2024, URL https://www.gurobi.com.
[44] Department for Energy Security and Net Zero. Prices of fuels purchased by manufacturing industry. 2025, Originally published 20 December 2012; last updated 27 March 2025, https://www.gov.uk/government/statistical-data-sets/prices-of-fuels-purchased-by-manufacturing-industry.
[45] US Energy Information Administration. Annual energy outlook 2025. Tech. rep., U.S. Energy Information Administration; 2025, URL https://www.eia.gov/outlooks/aeo/, Release Date: April 15, 2025.
[46] International Energy Agency (IEA). Gas Market Report, Q1 2025, IEA; 2025, URL https://www.iea.org/reports/gas-market-report-q1-2025, 2024 average TTF/European gas $11/MMBtu.
[47] International Energy Agency. The future of hydrogen: Seizing today's opportunities. Tech. rep., Paris: International Energy Agency; 2019, URL https://www.iea.org/reports/the-future-of-hydrogen, CC BY 4.0.
[48] IEA Bioenergy. IEA Bioenergy Annual Report 2023, Paris: IEA Bioenergy; 2024, URL https://www.ieabioenergy.com/wp-content/uploads/2024/06/Annual-Report-2023.pdf, Under the IEA Framework for International Energy Technology Collaboration; CC BY 4.0.
[49] Enerdata. Carbon price forecast under the EU ETS. 2023, URL https://www.enerdata.net/publications/executive-briefing/carbon-price-forecast-under-eu-ets.html.
[50] BloombergNEF. Europe's new emissions trading system expected to have world's highest carbon price in 2030 at €149. Bloom Rep 2025. URL https://about.bnef.com/insights/finance/europes-new-emissions-trading-system-expected-to-have-worlds-highest-carbon-price-in-2030-at-e149-bloombergnef-forecast-reveals/, Forecasts EU ETS II price of €149/t by 2030.
[51] Department for Energy Security & Net Zero. Powering up britain: Net zero growth plan. Policy paper, UK Government; 2023, URL https://www.gov.uk/government/publications/powering-up-britain/powering-up-britain-net-zero-growth-plan, Updated 4 April 2023. ©Crown copyright 2023. Licensed under the Open Government Licence v3.0.
[52] International Energy Agency. Energy technology perspectives 2023. 2023, URL https://www.iea.org/reports/energy-technology-perspectives-2023, Published 12 January 2023; CC BY 4.0.
[53] Department for Energy Security and Net Zero. UK emissions trading scheme (UK ETS): Technical guidance and tools. 2022, URL https://www.gov.uk/government/collections/uk-emissions-trading-scheme-uk-ets-technical-guidance-and-tools, Last updated 8 May 2025.
[54] Department for Energy Security and Net Zero. Greenhouse Gas Removals (GGR) Business Models: consultation. 2022, https://www.gov.uk/government/consultations/greenhouse-gas-removals-ggr-business-models.
[55] European Commission. Proposal for a regulation of the European parliament and of the council establishing a union certification framework for carbon removals. 2022, COM(2022) 672 final, https://climate.ec.europa.eu/system/files/2022-11/Proposal_for_a_Regulation_establishing_a_Union_certification_framework_for_carbon_removals.pdf.
[56] S&P Global Commodity Insights. Voluntary carbon markets. 2021, https://www.spglobal.com/commodity-insights/en/news-research/blog/energy-transition/061021-voluntary-carbon-markets-pricing-participants-trading-corsia-credits.
[57] Monitoring Analytics. 2022 state of the market for PJM, volume 2. 2022, https://www.monitoringanalytics.com/reports/PJM_State_of_the_Market/2022/2022-som-pjm-vol2.pdf, [Accessed: 2025-06-12].
[58] California ISO. Flex alert / emergency load reduction program archive. 2024, https://www.caiso.com/documents/grid-emergencies-history-report-1998-to-present.pdf, [Accessed: 2025-06-12].
[59] SMS Energy. Demystifying demand flexibility service (DFS) pricing. 2023, https://www.smsenergy.com/insights/demand-flexibility-service-dfs-pricing/, [Accessed: 2025-06-12].
[60] National Grid ESO. Demand flexibility service data portal. 2024, https://www.neso.energy/data-portal/demand-flexibility-service, [Accessed: 2025-06-12].
[61] Met Office. Met office integrated data archive system (MIDAS) land and marine surface stations data (1853–current). 2025, URL https://catalogue.ceda.ac.uk/uuid/220a65615218d5c9cc9e4785a3234bd0, [Accessed: June 10, 2025].
[62] European Parliament and Council. Decision (EU) 2015/1814 of 2 october 2015 on the establishment and operation of a market stability reserve for the union greenhouse gas emission trading system. Off J Eur Union 2015;L264:1–19, URL https://eur-lex.europa.eu/legal-content/EN/TXT/?uri=CELEX%3A32015D1814.
[63] European Commission. Report from the commission to the European parliament and the council on the functioning of the European carbon market. Off J Eur Union 2020. URL https://eur-lex.europa.eu/legal-content/EN/TXT/?uri=CELEX%3A52020DC0740, COM(2020)740 final.
[64] European Commission. Commission Implementing Decision (EU) 2023/386 of 14 march 2023 on the total number of allowances in circulation (TNAC) in the union registry. 2023, URL https://eur-lex.europa.eu/legal-content/EN/TXT/?uri=CELEX%3A32023D0386, COM(2023)386 final.
[65] US Department of Energy (DOE), Manufacturing and Energy Supply Chains (MESC). Replace conventional boiler with electric boiler | tipsheet 3. 2024, URL https://industrialapplications.lbl.gov/sites/default/files/pdf-embeds/IAC%20Decarb%20Tipsheet%203.pdf, Tip sheet (Energy.gov / MESC), Dated 1/11/24 on the document.
[66] US Environmental Protection Agency (EPA). Catalog of CHP technologies (full report). Tech. rep., U.S. EPA; 2017, URL https://www.epa.gov/sites/default/files/2015-07/documents/catalog_of_chp_technologies.pdf.
[67] National Energy Technology Laboratory (NETL). Cost of capturing CO2 from industrial sources. Tech. rep., U.S. Department of Energy; 2022, URL https://netl.doe.gov/projects/files/CostofCapturingCO2fromIndustrialSources_071522.pdf.
[68] Danish Energy Agency and Energinet. Technology data — Carbon capture, transport and storage. Tech. rep., Danish Energy Agency / Energinet; 2024, Version 0003 (amendment sheet: Apr 2024; prior updates Nov 2023; first published Nov 2021), URL https://ens.dk/media/4258/download.
[69] IEA Greenhouse Gas R&D Programme (IEAGHG) and CSIRO. Towards zero emissions CCS in power plants using higher capture rates or biomass. Tech. Rep., (Technical Report 2019-02). IEA Environmental Projects Ltd. (IEAGHG); 2019, Principal researchers listed in-report include Paul Feron, Ashleigh Cousins, San Shwe Hla, Ramesh Thiruvenkatachari, Kaiqi Jiang, Kaiqi Jiang, Rongrong Zhai; report citation given in the document, URL https://publications.ieaghg.org/technicalreports/2019-02%20Towards%20Zero%20Emissions%20CCS%20from%20Power%20Stations%20using%20Higher%20Capture%20Rates%20or%20Biomass.pdf.
[70] Hatta A, Consoli C, Seyyedi M. Cost of CO2 storage. Thought leadership, Global CCS Institute; 2025, URL https://www.globalccsinstitute.com/wp-content/uploads/2025/12/Cost-of-CO2-Storage-1225.pdf.